

Article

Lava Flow Hazard and Its Implication in Geopark Development for the Active Harrat Khaybar Intracontinental Monogenetic Volcanic Field, Saudi Arabia

Károly Németh ^{1,2,3,4,*}  and Mohammed Rashad Moufti ⁵

¹ Saudi Geological Survey, National Center for Earthquakes and Volcanoes, Jeddah 21514, Saudi Arabia

² Institute of Earth Physics and Space Science, Lithosphere Research Group, 9400 Sopron, Hungary

³ School of Agriculture and Environment, Volcanic Risk Solutions, Massey University, Palmerston North 4442, New Zealand

⁴ Istituto Nazionale di Geofisica e Vulcanologia, 40128 Bologna, Italy

⁵ Department of Mineral Resources Geology and Rocks, Faculty of Earth Sciences, King Abdul-Aziz University, Jeddah 21589, Saudi Arabia; mmoufti@kau.edu.sa

* Correspondence: k.nemeth@massey.ac.nz or nemeth.karoly@epss.hu; Tel.: +966-56-763-4717

Abstract: Harrat Khaybar is an active monogenetic volcanic field in western Saudi Arabia that hosts spectacular monogenetic volcanoes and a Holocene volcanic cone with extensive lava fields. The volcanic region is a subject of intensive land use development, especially along tourism ventures, where the volcanic features are the key elements to utilize for increasing visitation rates to the region. The youngest eruption is suspected to be Holocene and occurred fewer than 5000 years ago based on the cross-cutting relationship between the youngest lava flows and archaeological sites. Lava flows are typical, from pāhoehoe to ‘a’ā types with great diversity of transitional textural forms. Here, we recorded typical transitional lava flow surface textures from the youngest flows identified by digital-elevation-model-based terrain analysis, satellite imagery, and direct field observations. We performed lava flow simulations using the Q-LavHA plug-in within the QGIS environment. Lava flow simulations yielded satisfactory results if we applied eruptions along fissures, long simulation distances, and ~5 m lava flow thickness. In these simulations, the upper flow regimes were reconstructed well, but long individual lava flows were not possible to simulate, suggesting that morphological steps likely promoted lava ponding, inflation, and sudden deflation by releasing melts further along shallow syneruptive valley networks.

Keywords: pāhoehoe; ‘a’ā lava; spatter; lava tube; tumuli; scoria; pyroclastic; geodiversity; geoconservation; geotourism



Citation: Németh, K.; Moufti, M.R. Lava Flow Hazard and Its Implication in Geopark Development for the Active Harrat Khaybar Intracontinental Monogenetic Volcanic Field, Saudi Arabia. *Land* **2023**, *12*, 705. <https://doi.org/10.3390/land12030705>

Academic Editor: Wojciech Zgłobicki

Received: 1 March 2023

Revised: 14 March 2023

Accepted: 16 March 2023

Published: 18 March 2023



Copyright: © 2023 by the authors. Licensee MDPI, Basel, Switzerland. This article is an open access article distributed under the terms and conditions of the Creative Commons Attribution (CC BY) license (<https://creativecommons.org/licenses/by/4.0/>).

1. Introduction

Volcanic geoheritage is a recently recognized aspect of research to utilize volcanic features for geoconservation, geohazard education, and geotourism [1]. Volcanoes fascinate the public, and volcanism is of great interest among geological processes [2]. Volcanism is also one of the graphic examples of geohazards. Due to the growing human population, infrastructure, and urban expansion, geological processes have more direct impact on our society [3–8]. While volcanism has strong dark geocultural aspects through its destructive nature [9,10], it is also part of human civilization evolution as volcanoes provide good material to form valuable soil and become important regions for early human settlements [11–14]. Altogether, this forms a very strong heritage that is defined as volcanic geoheritage [15–19]. Volcanic geoheritage has also recently been treated, from volcano geology aspects, to provide a systematic framework to evaluate their values, compare their features, and see their geodiversity both from regional and global perspectives [20]. Volcanic geoheritage is clearly obvious in areas of active volcanism. The fascination with volcanic processes makes lands with no current volcanic activity important for the use of

old volcanic features or rocks to link them to active processes using this information in geoeducation and geotourism [21]. It is commonly recognized that regions with no current volcanic activity but located in volcanic terrain can form significant hubs for tourism and geoeducation [22–25]. Placing volcanic lands into a geosystem services concept, besides the obvious natural resource values that such volcanoes can offer (e.g., raw materials, mineral resources), their geoheritage appreciates increasingly [26–30]. In this scientific report, we explore the geoheritage aspects of a volcanic region in western Saudi Arabia that evolved over a long time and is suspected to have produced volcanic eruptions in the Holocene [31]. The main goal of this report, besides documenting the basic elements of the volcanic geoheritage of this region, is to test lava flow hazards, utilizing lava flow inundation modeling. Such modeling can provide a unique tool to incorporate in volcanic hazard education for use as a centerfold of the geoeducation concepts of this region for future geopark developments.

Saudi Arabia, in the past decade, has made significant investment to raise its tourism portfolio [32,33]. The Royal Commission for Al Ula (<https://www.rcu.gov.sa/en> accessed on 14 March 2023) is one of the flagship projects that is based on the cultural and natural heritage of NW Saudi Arabia, as one of the main target areas to promote tourism. The first attempt to estimate the geodiversity values of the major target areas within the Kingdom yielded valuable results to use for geoconservation and geotourism [34–36].

Tourism is also a recent concept within Saudi Arabia. A Scopus resource survey searching keywords such as “tourism” and “Saudi” returned 383 unique research papers. Interestingly, the number of publications about tourism subjects started to increase dramatically since 2012, indicating that tourism is, in general, a very new concept within Saudi Arabia. Tourism in general is based on religious pilgrimages such as Hajj and Umrah, primarily involving the region within the triangle of Al Madinah, Jeddah, and Makkah [37]. Saudi Arabia, similar to other parts of the world, has been hit strongly by COVID-19, and pilgrimage-related tourism has just recently recovered; but the post-pandemic has also created new opportunities to expand tourism activity beyond pilgrimage-related activities [38–40]. In current movements, tourism in Saudi Arabia is also promoted as a national identity that is linked to the diverse nature of the Arabian Peninsula [41,42]. Recent studies also show that Saudi Arabia has a strong domestic tourism sector that is beyond the common pilgrimage sector, and it is rapidly growing [43–45]. The general tourism is also expanding to occupy sectors of cultural activities [32,46–49], suggesting a very rapidly evolving sector of the Saudi society where niche tourism [50,51], hence geotourism, has a great future. The tourism sector within Saudi Arabia also embraced new and advanced approaches to explore the concept of tourism from very diverse aspects [52,53], which is very practical for geotourism developments.

Research work to evaluate the geoheritage values of the volcanic region of Saudi Arabia also culminated in various research reports and books that became widely used to explore the geotourism potential of the region [17,54,55]. Recent tourism development within the Kingdom has utilized the unique young volcanic landscapes of the Harrat Khaybar region by establishing a luxury ecotourism site named Khaybar Volcano Camp (<https://www.experiencealula.com/en/discover-alula/Khaybar/khaybar-heritage-tour/Khaybar-Volcano-Camp> accessed on 14 March 2023). The project is a successful venture bringing local and international visitors to a remote volcanic landscape that has received significant publicity since its establishment in late 2022 (<https://www.arabnews.com/node/2216726/saudi-arabia>, <https://www.arabnews.com/node/2141631/saudi-arabia>, <https://www.timeoutriyadh.com/hotels/khaybar-volcano-camp-opens-alulam>, <https://www.thenationalnews.com/travel/hotels/2022/12/12/khaybar-volcano-camp-opens-in-saudi-arabia-surrounded-by-lava-fields/>, <https://www.factmagazines.com/saudi-arabia/thrill-seekers-can-now-stay-at-khaybar-volcano-camp-in-saudi-arabia>, <https://whatsonsaudiarabia.com/2022/12/settle-into-the-luxurious-khaybar-volcano-camp-in-the-heart-of-lava-fields/>, all accessed on 14 March 2023).

While volcanoes are commonly viewed as long-lived conical geofoms that are active over a long time, there are also small-volume, short-lived volcanoes forming volcanic fields of monogenetic volcanoes [56]. Such monogenetic volcanic fields may be active over millions of years; their individual volcanoes are short-lived and new vents are likely to open in other places than where the last volcano formed. The Harrat Khaybar is one of such long-lived mature monogenetic volcanic fields [31,57]; hence, it is considered as an active volcanic field where young and well-preserved volcanic features make it a perfect representative candidate to explore from a geoheritage perspective. In this process, its youngest eruption site, Jabal Qidr, was nominated and then accepted as one of the International Union of Geological Sciences (IUGS) First 100 Geological Heritage Sites (https://iugs-geoheritage.org/geoheritage_sites/historic-scoria-cone-of-the-jabal-qidr/ accessed on 14 March 2023) [58]. Here, we explore the youngest volcanic features of this field and justify its geoheritage value within its geodiversity of monogenetic volcanism. We simulate first-time lava flow inundation in the region with an aim to provide key information for the lava flow emplacement mechanism that is supported by direct field observations. Based on this, we provide a comprehensive dataset that can be utilized within land use plans for future geotourism and geoeducation developments. Here, we provide an overview of the unique geosites of young lava fields and spectacular monogenetic silicic volcanoes to justify their high geoheritage values and global significance that can be the base of future geopark establishment.

2. Geological and Geoheritage Setting

Western Saudi Arabia is the home of at least nine distinct volcanic fields [55] that are delineated by the concentration of their source vents and the extent of the lava fields mapped with them. Among these volcanic fields—commonly referred to as harrats or black lava fields—Harrat Khaybar is one of the large fields by volcano numbers and surface area covered by lava flows (Figure 1). The two largest volcanic fields are located near the holy city of Al Madinah.



Figure 1. Microsoft Bing satellite image within QGIS shows the general landscape of the Arabian Peninsula. Note the dark zones in the western margin of the peninsula that are post-Miocene volcanic fields (harrats). Among them, Harrat Khaybar is located just north of Al Madinah city (red rectangle), and it is considered one of the largest and probably more geologically complex fields within the region.

Just south of Al Madinah, the largest volcanic field of the Arabian Peninsula, Harrat Rahat, is located. It consists of over 500 individual volcanoes such as typical scoria cones, lava spatter cones, and some trachytic lava domes and explosion craters [59–61]. While the field is dominated by basaltic volcanic products, trachytic lava domes and block-and-ash fans are known from its central part [62]. Among these silicic eruption sites, there is one dated to be about 4500 years old, concerning a young, Holocene, highly explosive and hazardous volcano [59] that was formed just before the Middle Holocene—Late Holocene subepochs boundary (4250 a b2k = 4250 years before the year 2000 (b2k) = 2250 BCE) and likely falls into the Northgrippian age [63]. Harrat Rahat is also the home of the youngest recorded eruptions within Saudi Arabia, which generated the 1256 CE Al Madinah eruption site through a 2.3 km long fissure that fed lava flows which reached the sedimentary basin where the city of Al Madinah is located today [64].

Just north of Al Madinah is the Harrat Khaybar, which is slightly smaller by surface area than Harrat Rahat. The volcanic field was formed in a long time over millions of years. The volcanic field hosts a larger number of silicic eruption sites than Harrat Rahat. Such silicic volcanoes are located in its central region, ranging from benmoreite to mugearite to potash rhyolites in composition [57]. The silicic volcanic landforms are tuff rings, single lava domes, and some block-and-ash fans. The common characteristics of these silicic eruption sites are their relatively simple stratigraphy framework, indicating relatively short-lived, “one-shot” volcanic eruption styles responsible for their formation [31]. As they also represent small volumes of eruptive products, they are monogenetic volcanoes, but are fed by shallower and more evolved magmas. The youngest eruptive products of the field form extensive lava fields, mainly in the central part of the field, with lava flows reaching over 60 km in distance from their sources, mostly toward the west. These young lava flow fields and their suspected source cone, Jabal Quidr, form the core of the geoheritage values explored and investigated for geotourism and geoeducation purposes [31]. The region has high geoheritage values as it hosts spectacular rare rhyolitic tuff rings and single lava domes such as Jabal Bayda and Abyad [65].

Saudi Arabia has no formal geopark established yet. However, at the project level, initial movements are clear and aim to establish geoparks in the Kingdom. As the volcanic fields, or harrats, are significant morphological elements of western Saudi Arabian landscapes, these lava-dominated volcanic terrains were suggested on several occasions to form the core conservation strategy and the geological basis of establishing geoparks [17,31,55,66].

3. Materials and Methods

In this report, first, we analyzed the terrain of Harrat Khaybar, utilizing terrain analysis tools with the QGIS (<https://www.qgis.org/en/site/> accessed on 28 January 2023) environment. To achieve this, we accessed the ALOS-PALSAR digital elevation dataset via the Alaska Satellite Facility (<https://search.asf.alaska.edu/> accessed on 28 January 2023) available for this region. These data provide 12.5 m resolution digital elevation information.

For identification of various generations of lava flows, we obtained Sentinel satellite images available from the Sentinel-HUB server (<https://www.sentinel-hub.com/> accessed on 28 January 2023) in preprocessed, terrain-corrected, and georeferenced format in the same coordinate and projection system as the DEM dataset. These maps are normally 13 m in resolution, but for detailed testing, we utilized 9 m resolution datasets as well. As the region is in an arid climate, it was easy to locate suitable views with zero cloud coverage, maximizing the information available from such data. We selected recent images dated 15 December 2022 with zero cloud coverage.

For the terrain analysis, we used the inbuilt SAGA GIS Next Generation plugin to perform basic terrain analysis. From the obtained data, we used the slope angle values to demonstrate the terrain topographic features. In addition, we used the SAGA GIS Next Generation (<https://saga-gis.sourceforge.io/en/index.html> accessed on 4 February 2023) plugin to determine the basic geomorphological features, geomorphons [67,68], using

default parameters for the calculations as the field visually shows very low variations in topographic features. Topographic variations were significant only where small-volume volcanic landforms occurred in the central regions.

We mostly used the preprocessed shortwave infrared composite (SWIR) images based on the 12, 8A, and 4 bands. SWIR data show if water is present in plants and soil, as water absorbs SWIR wavelengths. In SWIR images, the vegetation appears in shades of green, while soils and built-up areas appear in various shades of brown, and water appears black. Newly burned or barren land reflects strongly in SWIR bands, making them valuable for mapping fire damages or fresh lava flows. SWIR images show, very sensitively, the various lava flow types, with areas that are fresh and basaltic in composition being very reflective.

In addition, we also checked the false color composite image that is based on the 8, 4, and 2 bands. A false color composite uses at least one nonvisible wavelength to image Earth. The false color composite using near-infrared, red, and green bands is the most common and is used to assess plant density and health, since plants reflect near-infrared and green light, while they absorb red. Obviously, this is not the case for our study area as it lacks vegetation; instead, the reflectance difference distinctly shows the variation of young mafic lava flows and older lava surfaces, separating them sharply from loose-ash-covered terrains.

We also find it useful to distinguish lava flows using the Normalized Difference Moisture Index (NDMI), which is the ratio between the B8A-B11 values and B8A+B11 band values. The NDMI is used to determine vegetation water content and to monitor droughts. While the study area lacks vegetation, the variations recorded in such imagery reflect the geological architecture of the region. Low values normally correspond to barren soil, while higher values show more water. While this is, strictly speaking, relevant to vegetation cover, of which our research area has none, the color variation reflects the freshness of hard lava rock versus zones that are more granular, e.g., that already went through some desert weathering and/or represent ash covers where water loss (or quick accumulation) can be detected.

For the lava flow characterization of the youngest flows, we utilized the Microsoft Bing Satellite Image Repository as well as Google Earth Pro to locate key archaeological sites where human occupation features and desert kites are visible. We used this information to constrain the relative age of the lava flows. Desert kites are typical hunting features that are built as rock fences to divert wild game migration to a narrower flat area that is easily accessible, where some trap system captures some of the passing animals [69–72]. While the exact operation and functionality of these desert kites are under debate, in recent decades, thousands of such archaeological sites have been identified and described, from Central Asia to the Middle East and the Sahara [73–81]. Here, we compared the location of such desert kites in Harrat Khaybar with the lava flows associated nearby to them.

For the lava flow simulations, we utilized the Q-LavHA plugin of the QGIS software (<https://we.vub.ac.be/en/q-lavha>, accessed on 6 January 2023). Q-LavHA (Quantum-Lava Hazard Assessment) is a QGIS (Quantum Geographic Information System) freeware plugin which simulates ‘a’ā lava flow invasion probability from one or more regularly distributed eruptive vents on a digital elevation model. It combines existing probabilistic and deterministic models [82,83] and proposes some improvements to calculate the probability of lava flow spatial propagation and terminal length. The spatial spread is constrained by the probabilistic steepest slope following the approach of Felpeto et al. (2001). Corrective factors are included to allow the lava flow simulation to overcome small topographical obstacles and fill pits. The terminal length of the lava flow simulation can be determined based on fixed length values, a statistical length probability function, or based on the thermorheological properties of an open-channel lava flow, following the approach of the FLOWGO model [83]. As our study area is not strictly an ‘a’ā lava field with channel-fed lava flows ideal for applying Q-LavHA [84,85], the simulation results were treated as an indication of lava flow inundation proxy rather than a high-precision modeling tool. The reason we opted to use this simulation tool is that it is simple and

user-friendly, and it is incorporated in the QGIS freeware. In addition, it has also been applied earlier in similar volcanic systems, such as Harrat Khaybar [86]. While Q-LavHA indicates that it has been developed for 'a'ā lava flow modeling, we consider our field has such components, especially within the rubbly pāhoehoe lava field areas and other channeled nature, which we outline later. It is also evident that lava flows simulated recently by Q-LavHA are far more diverse than a sensu stricto 'a'ā lava, and, in many senses, share common characteristics that we observed in our field. Within the toolbox of Q-LavHA, we tried but have not taken into this report, FLOWGO as it requires numerous data inputs of the lava's estimated physical conditions that we can offer only in a highly speculative way. As our field is also located on a gentle sloping terrain (<5 degrees), we find that the best way to follow the simulation is to apply Euclidean simulation and long simulation distances (e.g., 10 times more than the measured flow runout distances) similarly to what was suggested in Paricutin, Mexico [87]. Though we have very limited direct information about the lava flow thickness, based on direct field observations, we opted to use 5 m average flow thickness with an extra 10 m buffer to allow the simulation to progress if the topography became too flat, as the simulation otherwise would terminate too early. We also acknowledge that our DEM has only 12.5 m resolution which limits the capture of fine details of micro-ruggedness of the terrain. While this is probably an advantage in the areas in proximal terrains where the complex lava accumulation zones created complex micromorphology, in distal areas, this resolution is not good enough to pick distinct shallow wadi networks that apparently capture thin (m range) lava flow lobes. Our null hypothesis was that the simulations will likely provide acceptable results within the proximal and medial settings, but further away, the reliability is expected to be pure. Based on these boundary conditions, we performed lava simulations as vents opening on the western and eastern sides of the summit region of the current Jabal Quidr cone. To perform this was an important step as the cone current morphology highly affects the initiation direction for any flow using any flow simulation packages. In addition, we performed point source flow initiation north of the Jabal Quidr, where mapping and satellite imagery confirmed young lava flow source regions. In addition, we used fissure simulations with 500 m eruption point spacing over fissures up to 3 km. Finally, we modeled lava flows initiated along a long fissure zone opening between Jabal Quidr and the northern emission zone, with the same 500 m eruption point spacing. We discuss the resulting simulations in the context of a volcanic hazard and hazard education perspective within the planned framework of geopark development initiative.

4. Results

4.1. Terrain Analysis

The 12.5 m resolution ALOS-PALSAR DEM was good enough to characterize the volcanic field morphology well. The generated contour map with 50 m contour density with a combination of topography-enhanced DEM color maps over hill shade with five-times exaggeration provided a good visual image of the entire field, highlighting its very gentle morphology (Figure 2). This monotone landscape became more complex only in the center part of the field (Figure 2). This is clearly visible in the generated east-to-west and north-to-south cross-sections (Figure 3). The low slope angle is apparent in the cross-sections in the distal part of the field, suggesting that the lava flow simulation within the available map resolutions likely needs to be adjusted to flat terrains (e.g., using increased simulation distances).

The slope angle map for the whole field showed very well that the region is flat, but with a gentle sloping nature. The slope map in the central region of the field, however, showed steep-sided fresh volcanic cones forming the core of the volcanic fields (Figure 4); the steeper the slopes, the younger the volcanic landform appeared to be in the field. Interestingly, within the steep cones, the terrain still showed a remarkably flat nature. The intercone areas just dissected a very shallow gully network that is difficult to visualize within the available DEM resolution.

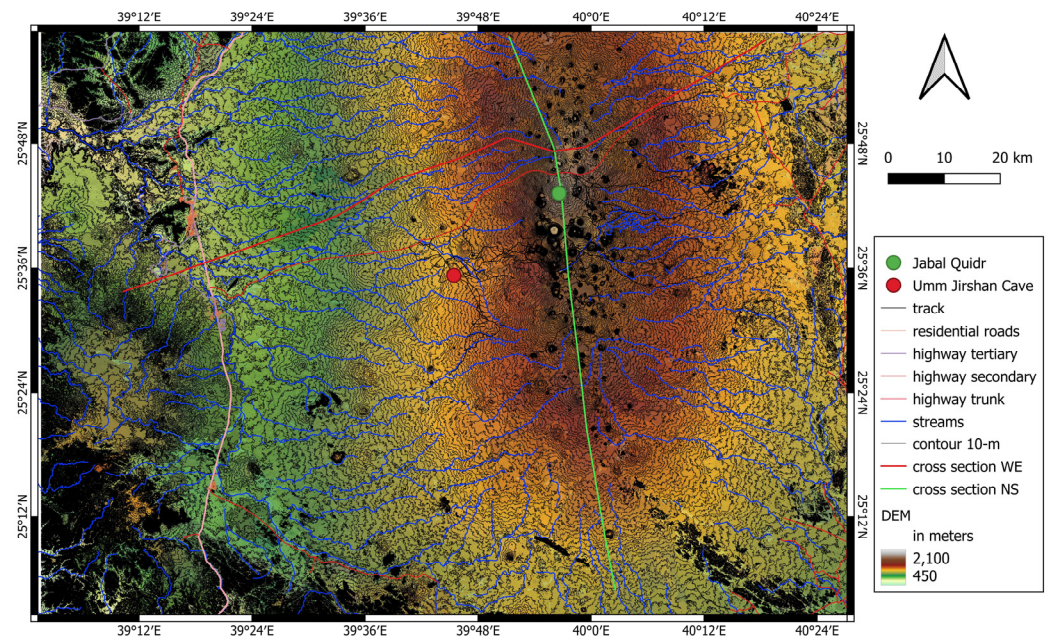


Figure 2. Digital terrain model based on the ALOS-PALSAR 12.5 m resolution elevation data over the geological map of the region. Young lava flows are clearly visible in the underlying map. Note the gentle sloping terrain and the dorsal-ridge-like feature upon which the volcanoes sit. Cross-section lines are marked on the map, and cross-sections are shown in Figure 3.

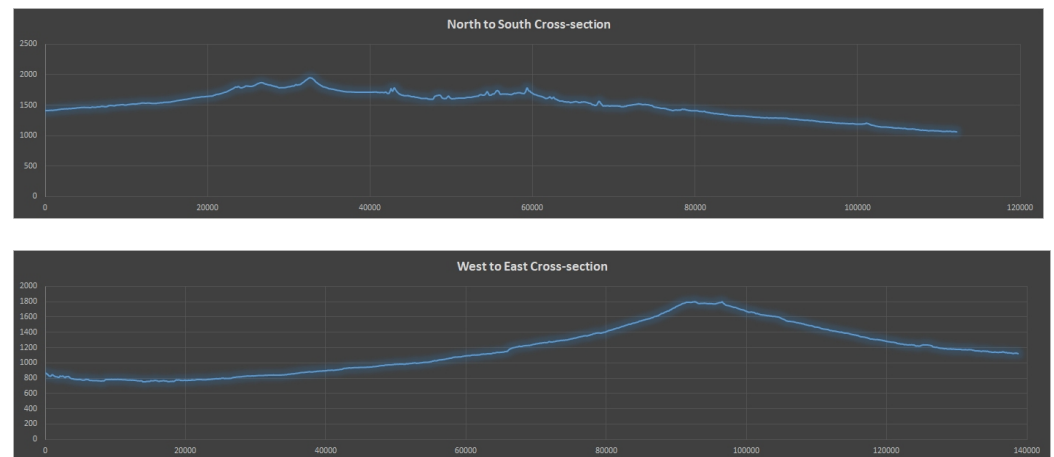


Figure 3. Topographic cross-sections generated in QGIS along the two N–S and W–E transects shown on Figure 2. Note the gentle sloping terrain and the near-steady-elevation dorsal range of vents.

Applying the geomorphon calculations, the above outlined terrain characteristics are also evident. The dominant landform types of the central part of the field are “slopes”, gently sloping (<2 degrees) but generally flat landforms (Figure 5). Hollows, foot-slopes, valleys, or depressions were recognized only in the central areas, where the relative morphology between cones and their bases was slightly more rugged (Figure 5). Along areas in the western side of the central cone zone, slight steps can be recognized in the morphology. Just east of this region, older and flatter lava flows tend to occupy the region where the largest known lava tube in the field is located. It is interesting that geomorphon calculation did not pick up characteristic valley networks even within those areas where ephemeral fluvial networks are mapped and known. With the given 12.5 m resolution DEM, the terrain analysis provided a gentle landscape for most of the volcanic field that has a gentle dip away from its north–south-trending dorsal zone. To further explore the terrain characteristics, satellite images were utilized.

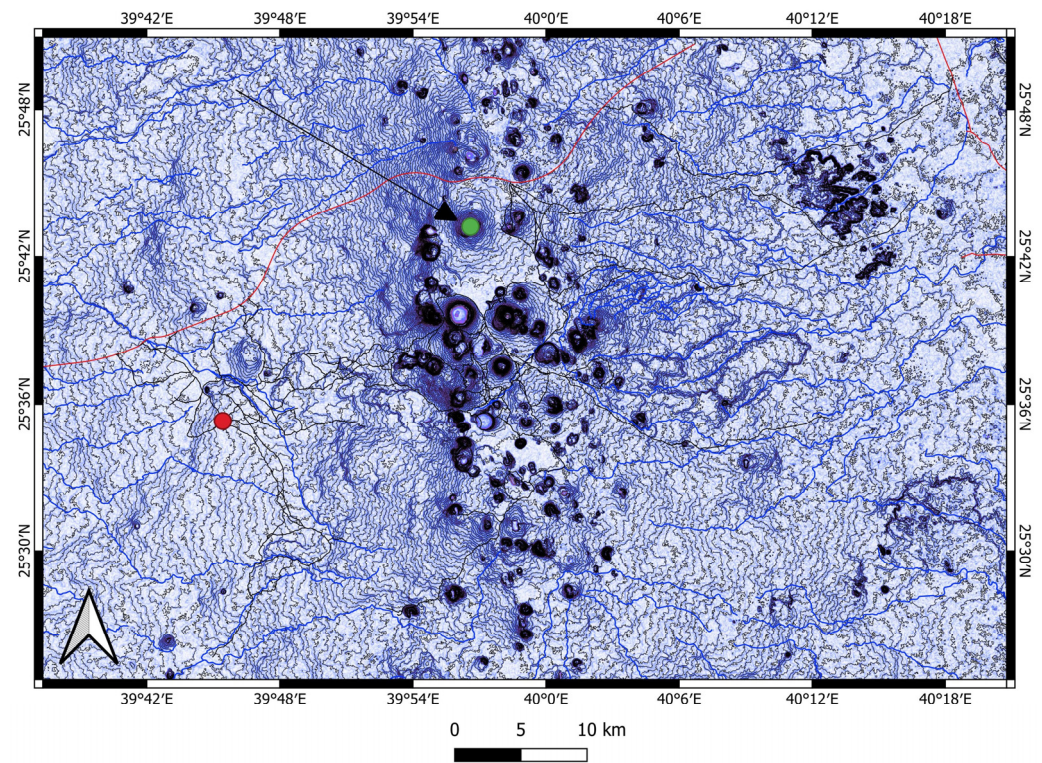


Figure 4. Slope angle map indicates a morphological step just west of the vent zones. Contour intervals are 10 m. The arrow points to Jabal Quidr (green circle). The position of Umm Jirshan Cave is marked by a red circle. The sealed road is a red line, while dirt roads are marked with black lines. Temporal stream networks are shown with blue lines.

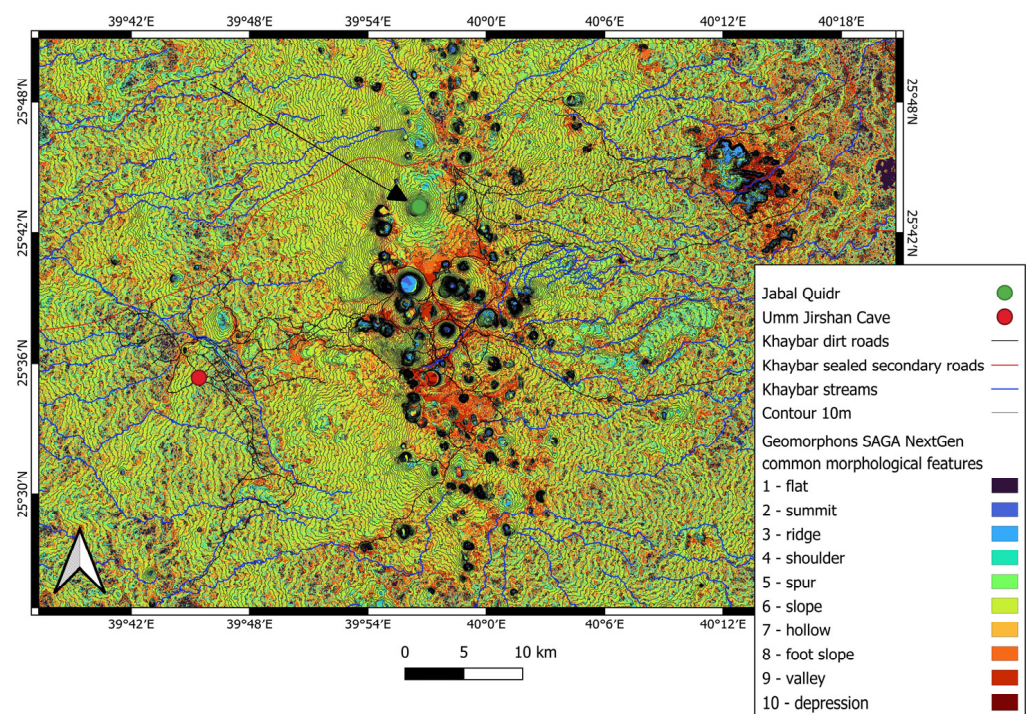


Figure 5. Geomorphon map of the central part of the field, showing the gentle sloping region away from the dorsal ridge of the vents in the central regions. Contour intervals are 10 m. The arrow points to Jabal Quidr.

4.2. Satellite Imagery

On the Sentinel SWIR image, the central part of the terrain distinctly shows the younger lava flows (Figure 6). Loose ash and lapilli fields are normally shown differently, reflecting their dry nature. On this image, the darkest lava flows are indistinguishable from each other, suggesting their common age and textural features (Figure 6). The same pattern can be observed within the moisture index map, highlighting the young nonweathered lava surfaces distinct from the rest of the field. This image also indicates that most of the young lavas represent a similar age and textural range (Figure 7).

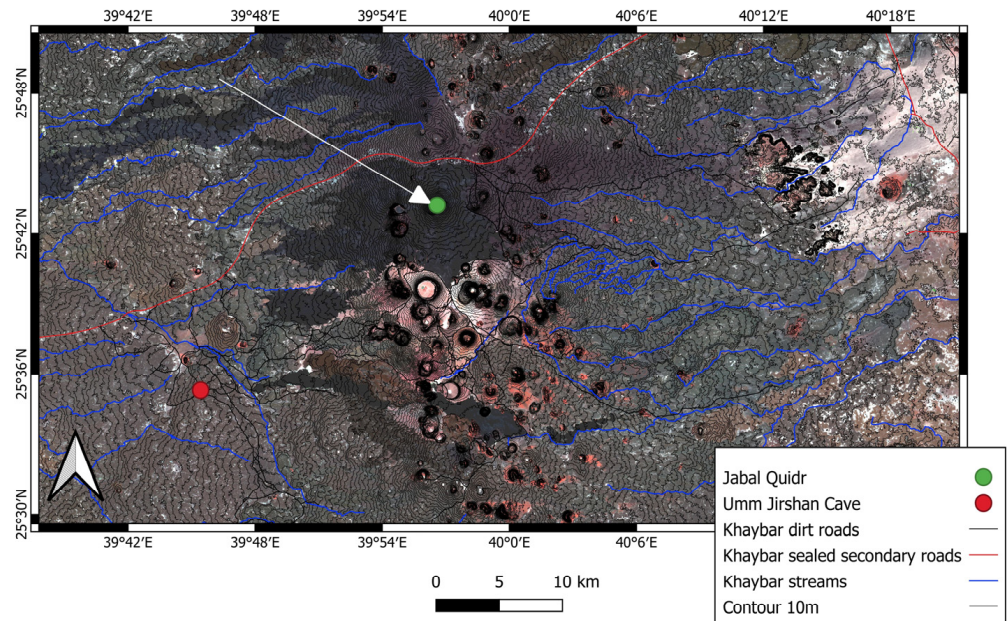


Figure 6. SWIR Sentinel satellite image showing the young lava flows clearly (dark) and their separation from pyroclast-filled zones (pinkish). The arrow points to Jabal Quidr.

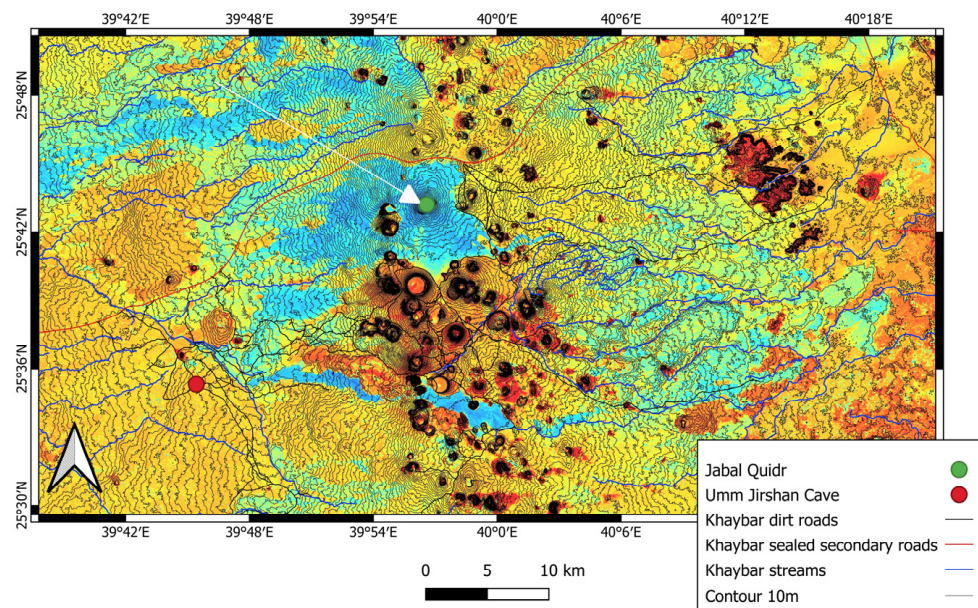


Figure 7. Moisture index map based on a Sentinel image of the center part of the volcanic field. Dark red/orange zones represent low moisture content (e.g., dry ash), while blue regions indicate smooth and moist surfaces, such as young lava flow axes. An arrow points to the location of Jabal Quidr.

4.3. Lava Flow Surface Texture

Lava flow surface textures were observed from helicopter flights and on the ground. This dual approach was necessary, as on the ground, the location of various textural boundaries were not as obvious as after a fly over.

In the proximal settings close to source vents, the lava flow was typically pāhoehoe, with thin layers of glassy but vesicle-rich surfaces. In the larger cones' flanks, convoluted lava flow channels commonly formed complex lava surface textures or regions where only thin layers of lava were preserved, such as on the flank of Jabal Quidr (Figure 8). This convoluted surface texture manifested well in rugged surface areas in the proximal areas, especially where the steep cone flank facilitated lava flow movement promoting destruction of initial colling surfaces. In these areas, the formation of a significant tube network, or ponding, was not possible, as lava just cascaded down. The result of these cascaded ripped flow crusts was the formation of some channelized zones right at the feet of the major cones such as Jabal Quidr (Figures 8 and 9). Further away, ponding became more apparent, as in the gentle sloping regions, flow movement must have slowed down to allow the formation of chilled crust that showed up as shiny plates on the air photos (Figure 8).



Figure 8. Jabal Quidr's eastern side with the complex lava flow field and the deep crater of the cone. Lava flows were partially fed from overflow of the crater and some side fissures. Lava flow outpouring and draining triggered crater floor collapse and the generation of the deep crater. The crater is about 250–300 m across.

Lava flows further away seemed to be captured in shallow morphological regions, including wadis (dry valleys), where they formed flat-topped lava channels such as those developed on the eastern side of the Jabal Quidr cone (Figure 9). Lava flow textural changes are very clearly visible on the eastern side of Jabal Quidr, and provide vital information to justify the model used for lava flow simulations (Figure 9). Along the eastern foothills of Jabal Quidr, the lava flows clearly form relatively thin (dm-scale) layers of lava that are vesicular, and the vesicles form zones from the base to the top of the flows (Figure 10).

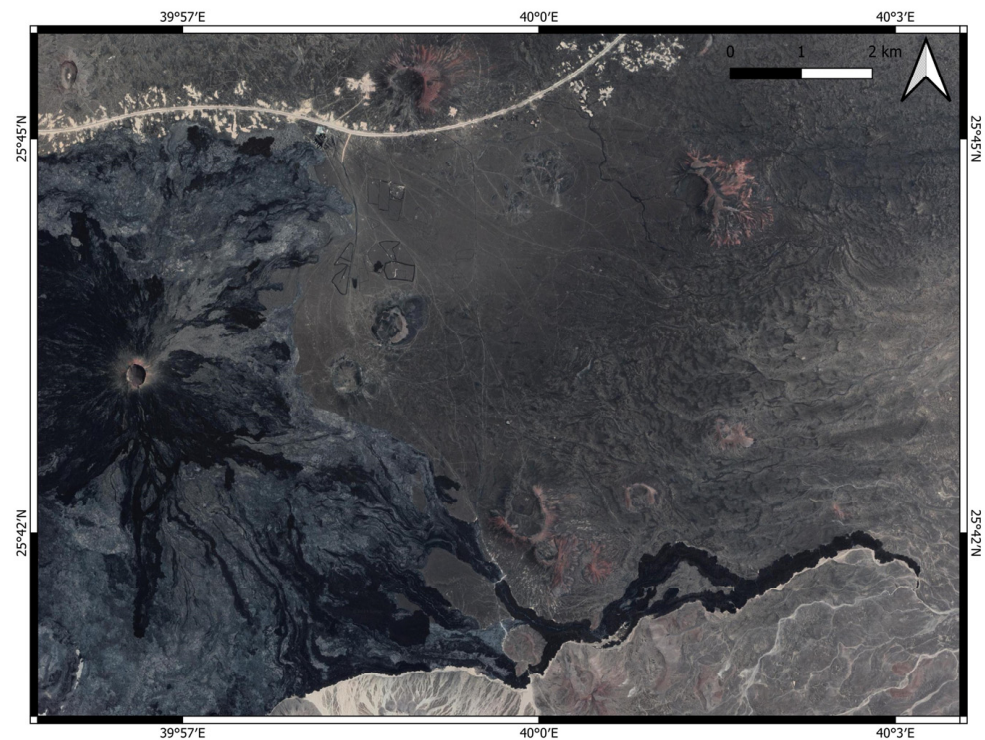


Figure 9. The eastern zone of Jabal Quidr on a Sentinel satellite image with a characteristic lava channel that transforms into a bubbly pāhoehoe from the inflated tube-fed zones in the foothill area. Lava is diverted toward the south to pass the pre-eruptive obstacles formed by older cones. An ash plain covers the pre-eruptive landscape, indicating that the lava flow emplacement post-dates the major explosive phase and scoria cone growth of Jabal Quidr.



Figure 10. The eastern foothill of Jabal Quidr (about 2.3 km from source) with inflated, vesicular pāhoehoe sheets.

The outer part of the lava flows is glassier, and smoother pāhoehoe surface textures are apparent in areas where the slope angle changes from the steep edifice part to the foothill zones, suggesting temporal lava ponding where incoming lava forms convoluted wrinkle

textures on the growing lava pond (Figure 10). In these areas, localized inflation features generated uplifted convex upward zones such as embryonic tumuli [88] (Figure 10). In the axis of the main flow paths, such tumuli suffered opening along dm- to meter-scale long cleavages, promoting deflation and collapse of the relatively thin roof of the tumuli (Figure 10).

In the proximity of lava spatter cones [89], the rapid accumulation of pyroclasts generated clastogenic lavas that also intermingled with fresh flows initiated from the fissures. These areas formed very complex lava surface textures characterized by pāhoehoe roopy lavas and thin chilled-crust-bounded dm to meters wide and several tens to hundreds of meters long lava tubes (Figure 11). These features clearly form positive, concave-up micromorphology, indicating rapid flow movement of low-viscosity melt developing thin crusts that are gradually vesiculating but still holding the melt together as a deformable skin/crust-bounded narrow channel (Figure 11).



Figure 11. Narrow, partially unroofed flow channel at the foot of a lava spatter cone. The channel is about 2 m wide.

These narrow lava channels often appear to be unroofed in areas where the spatter cone edifice of the fissure-fed zones is steep or where the slope angle of their accumulation surface is changing as a reflection of the changes of velocity and dragging power of the moving melt within the self-developing tube (Figure 11).

Similar unroofing is inferred in those areas where large volumes of magma ponded just in the vicinity of the main feeding vents that are normally fissure-fed spatter cones. Where large volumes of lava gushed out from the vent, their movement slowed down in areas where slope angle reduced dramatically. Such morphological change prevented the lava movement, further prompting lava ponding, inflation, and crust formation. In these zones, thin but vesicular crust developed that did not produce shiny outer flow surface textures. This is inferred to be caused by the combination of the active and intense degassing of the incoming volatile-rich melt and its vigorous movement that placed mechanical stress on the formation of these inflation zones. These zones are normally mapped about a few hundreds of meters away from the source fissures and can be traced as rough-surface-textured lava fields. These zones also exhibit broad areas where deflation took place that is inferred to be driven by the sudden increased force of overinflated ponded lava that then suddenly emptied. These deflation zones are commonly observed in areas where the flow channel has some morphological steps. By reaching a critical ponded volume, the

inflated zone breached, emptying the lava downflow. In these deflation zones, vesicular lava crusts form a chaotic “clastic” zone of rubbly pāhoehoe. Interestingly, in these zones, the surface textures of each curved crust exhibit significant vesicular texture and lack of smooth shiny pāhoehoe surface forms, indicating the presence of still-active volatile-rich lava to prevent the formation of smooth surfaces (Figure 12). The deflated and crumbled flow surfaces also amalgamated with dm to meter wide tubes, indicating incoming fresh flow, even at the time of deflation and roof collapse of these zones (Figure 12). Based on the presence of only thin crusts (cm-scale), it can be inferred that the lava system must have been very rapid-moving, changeable in incoming flow locations and places where breaches initiated, not allowing time to settle and cool the main lava body to develop thicker crust and more regular surface texture. This complexity indicates fresh volatile-rich magma input, low-viscosity lava involvement, and high flux rate. Similar lava flow emplacement and resulting surface textures were reported from recent lava flows that were created by high-lava-flux fissure-dominated eruptions such as those in the Holuhraun lava field in Iceland in 2014–2015 [90].



Figure 12. Thin, highly vesicular lava crusts in proximal settings forming a complex collapsed roof zone of pōnded lava. Individual lava crust plates are about a meter across.

In the medial flow fields, the lava flow surface texture commonly changes to more well-defined shiny chilled-top flows to wide channel-like zones where rubbly pāhoehoe form flow fields resembling clastic rubble of fragmented lava crusts and completely abraded cauliflower-shaped rugged cm to dm size fragments (Figure 13). It seems that these rubble zones are similar to the main axis of flow movement as they exhibit complex channel networks such as channelized lava flows of higher-viscosity intermediate flow types (Figure 13). These flow channels are commonly encountered by smooth-topped zones of lava with chilled crusts that are occasionally fractures due to the mechanical stress of the flow propagation (Figure 13). While there is some general trend of the appearance of these axial smooth-topped zones and the rubbly channelized flow paths, they are not entirely systematic, such as has been observed in many large and long lava flows in Harrat Rahat [91]. There are examples where the rubbly flow seemingly forms the distal lobes of channelized and shallow wadi-captured lavas in the distal areas and the terminus of the flow itself (Figure 9), smooth, tube-like flow channels are also observed in distal regions, completely occupying the otherwise shallow (less than 5 m deep), localized, dry valleys, with distinct inflated smooth-topped tubes that are only partially surrounded by some eroded rip-up clasts of flow-topped plates (Figure 14). This is inferred to be the result of

the complex interplay of lava flux, the dropping temperature of the flow, its heat retention, and the very shallow valley network.

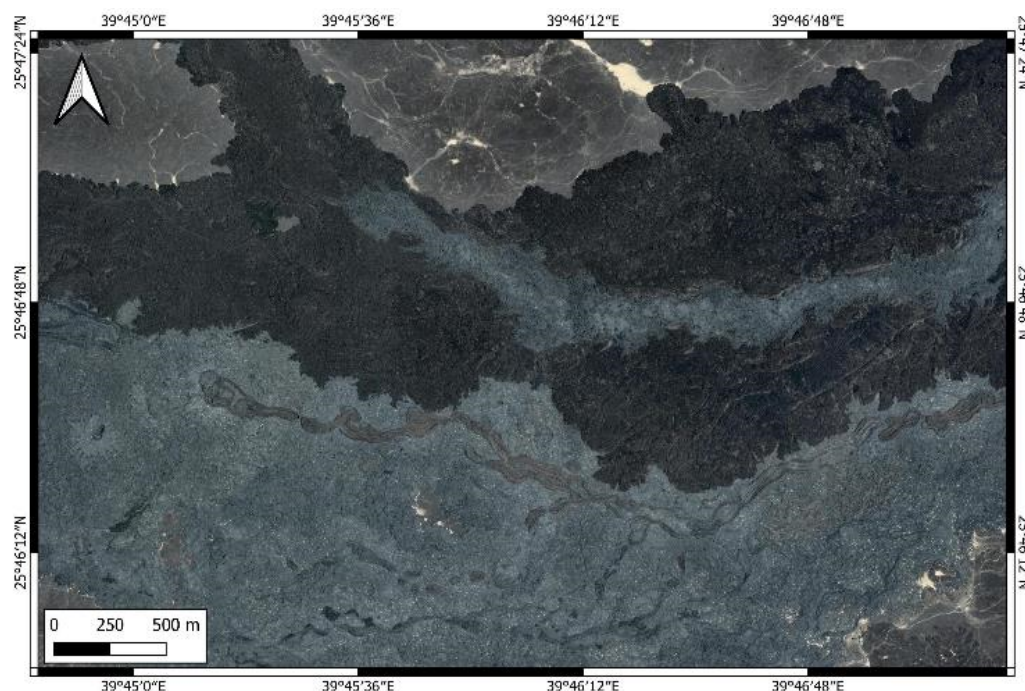


Figure 13. Complex lava flow path in medial section of one of the youngest lava flows. Note the complex rubble and shiny, shelly pāhoehoe surfaces as well as the narrow, thin-crust flow channels, all indicating a dynamic lava flow emplacement environment where ponding, inflation, deflation, and localized and general surface crust breach generate a complex lava flow surface texture.

It is apparent, based on the surface textures of the youngest lava flows, that tube formation is taking place mostly in those areas where slope angle changes of the emplacement area dropped to promote lava flow ponding. Such ponding first occurred near the source edifice foothills. Further ponding is recognized in the western regions just about a few km from the main axis of the vents of the central part of the volcanic field. In these areas, the lava flows tend to form thick piles that are perfect for retaining heat and keeping lava molten for a long time. It seems that these ponded zones played a critical role in the final lava flow distribution and flow direction control at Harrat Khaybar, similar to what was observed in the Icelandic 2014–2015 Holuhraun lava flow field evolution [90]. A fine example for this region, where older lava flows are known to host large, long lava tubes, is the Umm Jirsan, which is Saudi Arabia’s longest lava cave [92]. The cave is about 1500 m long and 45 m wide, with a maximum height of 12 m [93] (Figure 15), and forms the core tourist attraction of the region around geotouristic and geoeducation programs planned to be built and incorporated in future geopark developments. This lava cave is clearly part of a large lava tube, a main artery of lava flow transportation from its former source that developed over the topographical step west of the main vent axis of the field, indicating long-lasting stable conditions to maintain the formation of this large tube. Similar tubes are expected to form in the youngest flow fields and likely acted as “secondary” flow initiation points to effectively transfer melt to more distal regions of the field. This is vital information for interpreting the lava flow simulations later.



Figure 14. Tube-fed hummocky surfaced lava flow arm that is emplaced in a very shallow wadi about 45 km away from its source from the fissure vents north of Jabal Quidr. Photo was taken from a helicopter looking upflow toward the NE. Note the very flat, but gentle, sloping topography across which the lava flow spreads. The narrow neck of the lava flows in the foreground is about 75 m wide, and its location is $25^{\circ}39'13''$ N $39^{\circ}30'18''$ E.



Figure 15. Umm Jirsan ($25^{\circ}35'18''$ N $39^{\circ}45'25''$ E), which is Saudi Arabia's longest lava cave. It is about 1500 m long and 45 m wide, with a maximum height of 12 m, and forms a major tourism attraction site and a globally significant geosite.

4.4. Desert Kites and Human Occupation Sites Constraining Holocene Volcanism

There are very limited and conflicting data available to determine the age of the volcanism of Harrat Khaybar [31,57]. It is evident that the region must have had very young eruptions producing long lava flows as they are distinctly different from other lava features in any satellite imagery available. There are various arguments placing these volcanic events in the Pleistocene or Holocene, but recent satellite image survey and field visits indicate that one of the major, over 100 km long, lava flows with clear young surface textures on satellite images is covering archaeological sites. Desert kites are common archeological features of Harrat Khaybar [69]. While it is not evident what they are, more evidence points to their role as ancient hunting traps. It is known that the Arabian Peninsula experienced at least 21 pluvial periods since 1.1 Ma, when precipitation reached the value of 300 mm/y [94]. While the Holocene is a dry period within this timeframe, recent research provided vast evidence that the Arabian Peninsula was habitable between 9 and 7 ka, and with short dry spells, the region was likely wetter than today until about 5.4 ka, until the onset of the “dark millennia”, when population decline affected the entire region, leaving behind no archaeological evidence of significant human occupation sites in inland Arabia [95]. Works outlined that game migration in the region during a pluvial climatic period followed vegetation zonation that was highly influenced by the former fluvial networks formed within shallow valleys between smoothed and weathered older Pleistocene lava flows [77]. Triangle-shaped (in map view) rows of stones of over a hundred meters long built in flat and smooth areas that were open savannahs during pluvial times guided game to specific locations where other trap mechanisms disoriented them, causing them to fall off cliffs or just enabling simple ambush by hunters. In Harrat Khaybar, many of such desert kites identified in the distal, low-lying areas of the volcanic field and located in areas functioned as broad, soft, sand-filled valleys (Figure 16). These desert kites commonly face their “mouth” toward broad open spaces, likely bordered with trees and partially filled with streams (judging from the silt deposits associated with such zones). There are desert kites that are partially covered by the young-surface-texture lava flows (Figure 16). Alternatively, there are desert kites that are faced toward rugged fresh lava flow lobes along the terminus of the lava flows (Figure 17) that are unlikely to be places any game migration would progress. On other hand, the same locations prior to lava flow emplacement are locations with broad, probably vegetated savannahs ideal for migrating game (Figure 17). If we accept that the lava flows are younger than the archeological occupational sites, their age could be as young as 4500 years based on the general settlement history of the region over time. This is in good concert with the suspected eruption age of Jabal Quidr around 1000 CE, informally agreed upon by experts. The surface textures of the lava flow in satellite images also indicate similar patterns, as has been documented from the nearby Harrat Rahat where a historic eruption took place in 1256 CE, and other historic lava flows are also determined to be Holocene in age. Harrat Khaybar, in this sense, is an active volcanic field, and the current geopark development of the region needs to embrace this fact in their geopark management, land, geoeducation, and geotourism strategies.

4.5. Lava Flow Simulation

For the lava flow simulations, we estimated 5 m lava flow thickness as an average value. This is probably an overestimation in distal areas, while an underestimation in proximal ponded zones. We adjusted the Q-LavHA with a 10 m thickness buffer to allow the simulation progress in the very marginal values as recommended in the program descriptions. The simulation distance (L) value was selected to be in the range of more than 10 times the measured flow length. In an extreme case, such as 100 km (100,000 m), this is yielded to be in the range of hundreds of kilometers. We ran numerous simulations and visually compared the results of the probability fields of lava inundation with the general pattern of the youngest lava flow distribution patterns. We used every area where nonzero probability of lava inundation was calculated to show the region where lava inundation is expected without dealing with the actual probability values. In short, with this approach,

we were able to delineate areas whereby, given the input parameters, we expect lava to be covering the surface. In this way, we tested lava emission points and various fissures. In the first set of simulations, we tested single point sources in the eastern summit region of the Jabal Quidr cone (Figure 18). This simulation yielded lava-flow-covered areas significantly smaller than what we experienced in the field by mapping the region lava flow coverage. In a single simulation from a single point, it was not possible to recreate flow patterns visible in this part of the cone; however, even a single simulation provided a good coverage and trend of the flows observed. This indicates that, probably, multiple (but not large numbers) flow emissions could successfully create the flow field we see preserved today in the case of future eruptions.

A similar single point simulation just on the western side of the summit region of Jabal Quidr yielded a good lava flow inundation pattern that fits well with the observed lava flow distribution pattern (Figure 19). In these areas, longer simulation distances were selected as young lava flows seemingly reach far from the source vent in the western regions (Figure 19).

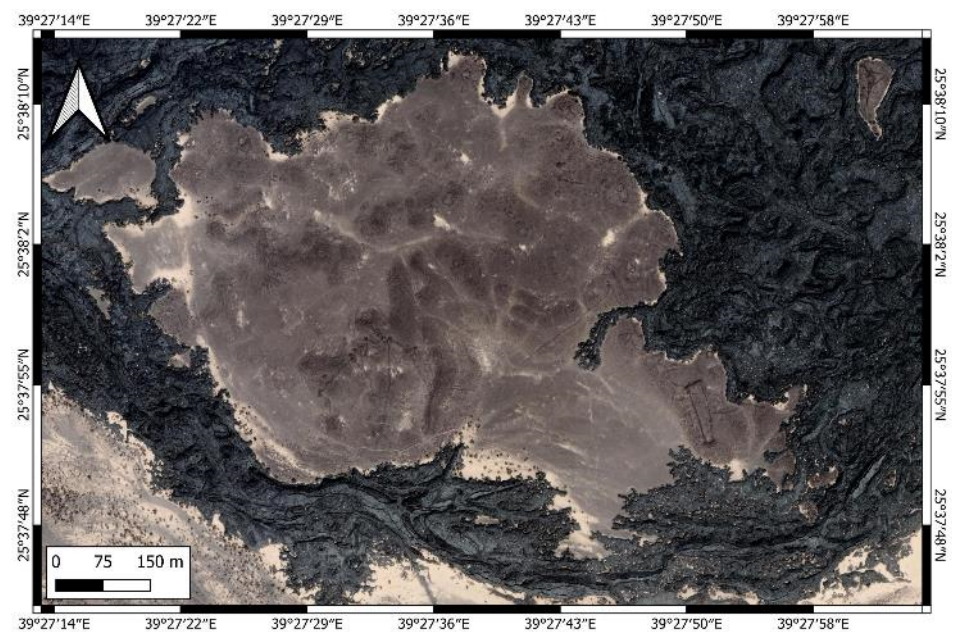


Figure 16. Smooth-surfaced old surface surrounded by rugged fresh lava flows locking desert kites in that are unlikely places to erect, as the enclosed areas are unlikely regions for free game migration as they are blocked by the lava flows.

Interestingly, in this site, a single simulation generated a good match with the observed flow pattern. To generate a better match, a few extra lava flow initiations would be required within the same area. To generate the complex lava flow inundation in the west and east of the current Jabal Quidr requires that flow is somehow able to pass the edifice, avoiding its obstacle effect. This is inferred to be possible if the lava is initiated from the summit region through fissures cutting through the edifice itself. During site observation, signs of such facies architecture are noted as a possible scenario.

In either simulation, however, no lava inundation was simulated that would cover the areas north of Jabal Quidr. To overcome this issue, we applied fissures as a main source region to initiate lava flows in that area. These initial conditions are realistic, as field survey confirmed that aligned fissures and associated lava spatter cones are typical in that area and form a complex proximal vent–flow field. In this simulation, we used a fissure that had the same orientation as the main vents in the dorsal range, and we applied about 2–3 km in length of fissures where the presence of vents is confirmed. Along this fissure, we applied 500 m active vent spacing and up to 500 km simulation distances. The lava flow inundation probability map showed a remarkably correct coverage of lava cover (Figure 20).

Finally, we tested complex and long fissure behavior (Figure 21). We simulated lava flow inundation along a long single fissure that connects the Jabal Quidr to the northern spatter cone chain. This simulation used long simulation distances and 500 m vent spacing over a fissure 20 km long. While this seems a very prominent feature, field observations justified that it is feasible, as active young vents that represent high stratigraphy position (hence, young age) are clearly traceable along this distance.

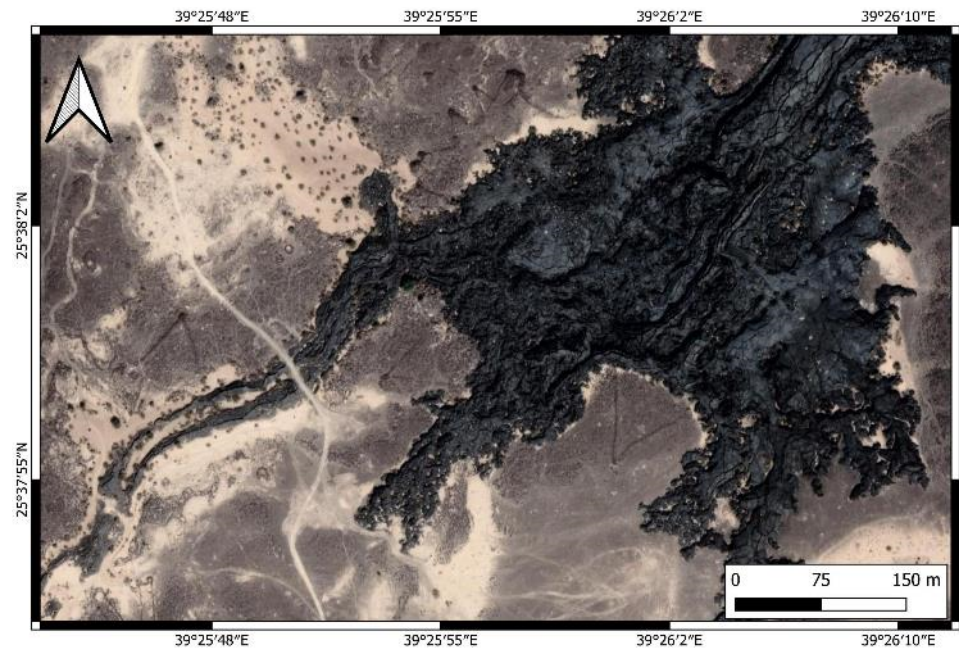


Figure 17. Two desert kites closely facing toward the terminal zones of young lava flows are unlikely places to set up game traps as the rugged surfaced lava flow is not a place where animal migration is expected. This is indirect evidence that the lava flow was emplaced after the desert kites were constructed.

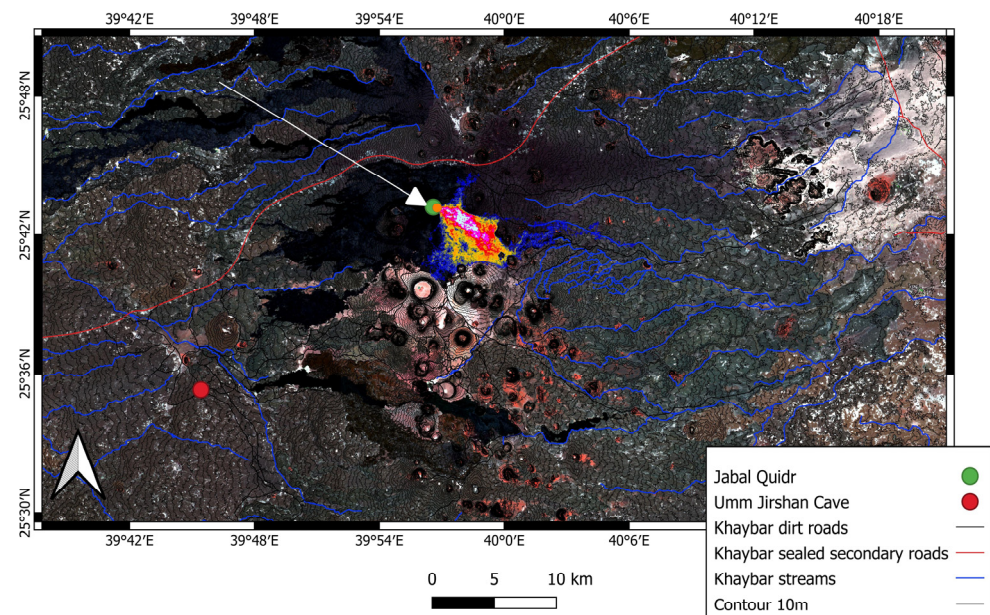


Figure 18. JQ1 vent (green dot just below the summit of Jabal Quidr marked by green dot) using 5 m (10 m) Euclidean simulation with 80 km simulation distance. Results overlay the SWIR satellite image of the region. Red dots mark the Umm Jirshan lava tube. The stream network is marked in blue, while a sealed road crossing the region is marked by a red line (data are from Open Street View).

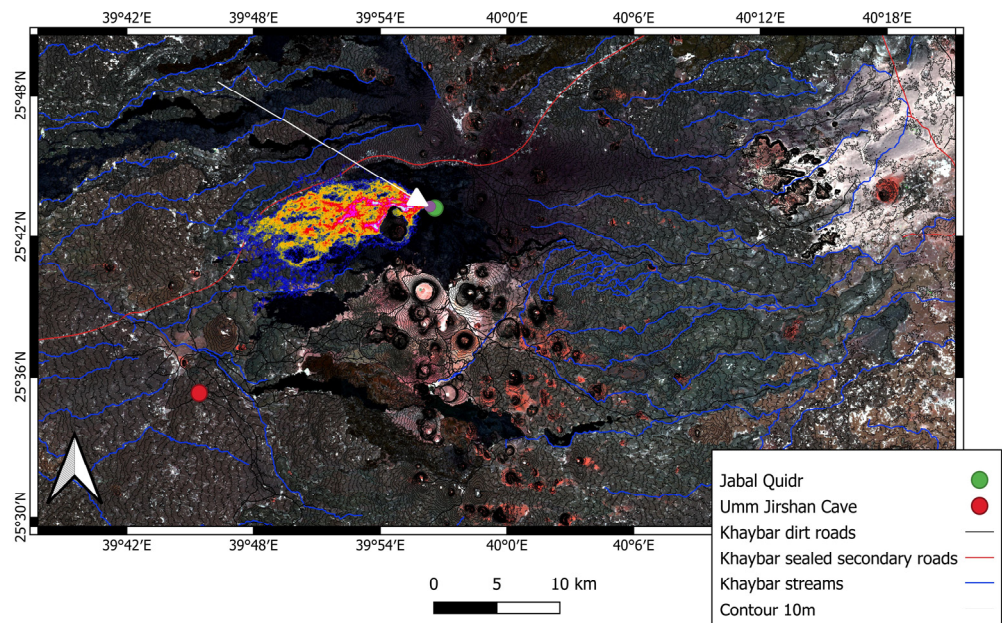


Figure 19. JQ2 (green dot just below the summit of Jabal Quidr, marked by purple dot and a white arrow) using 5 m (10 m) Euclidean simulation with 500 km simulation distance. Results overlay the SWIR satellite image of the region. Red dots mark the Umm Jirshan lava tube (data are from Open Street View).

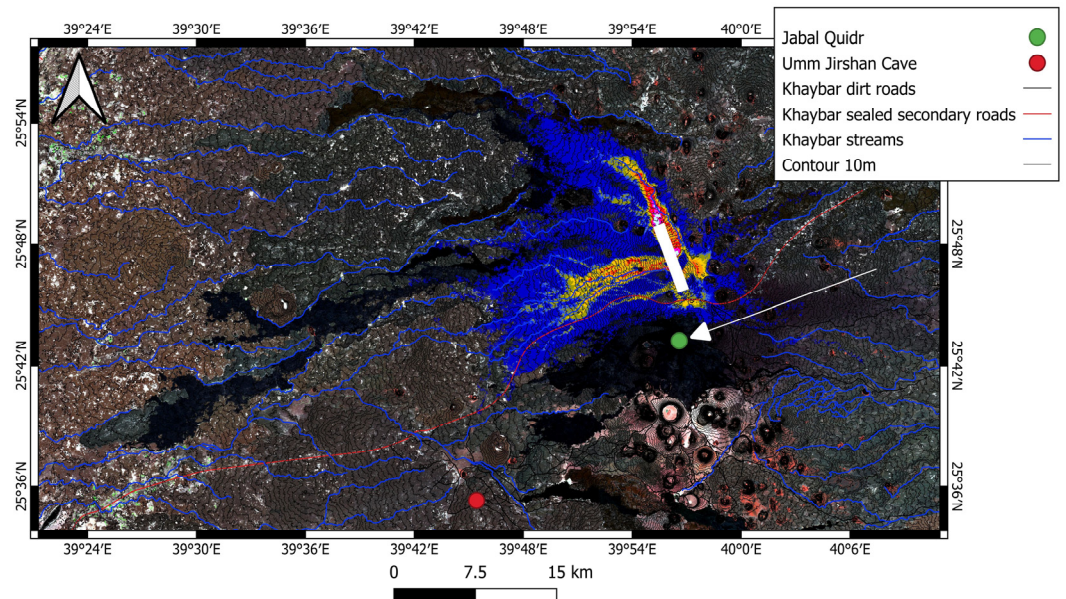


Figure 20. JQ fissure simulation with the same lava thickness parameters and 500 km simulation distances yielded a good match with the lava flow distribution pattern observed but failed to let the lava flow inundate the distant areas. Lava flow inundation reached only those zones observed in the field that acted as ponded regions. The green dot marks Jabal Quidr, while the red dot is the location of the Umm Jirshan lava tube.

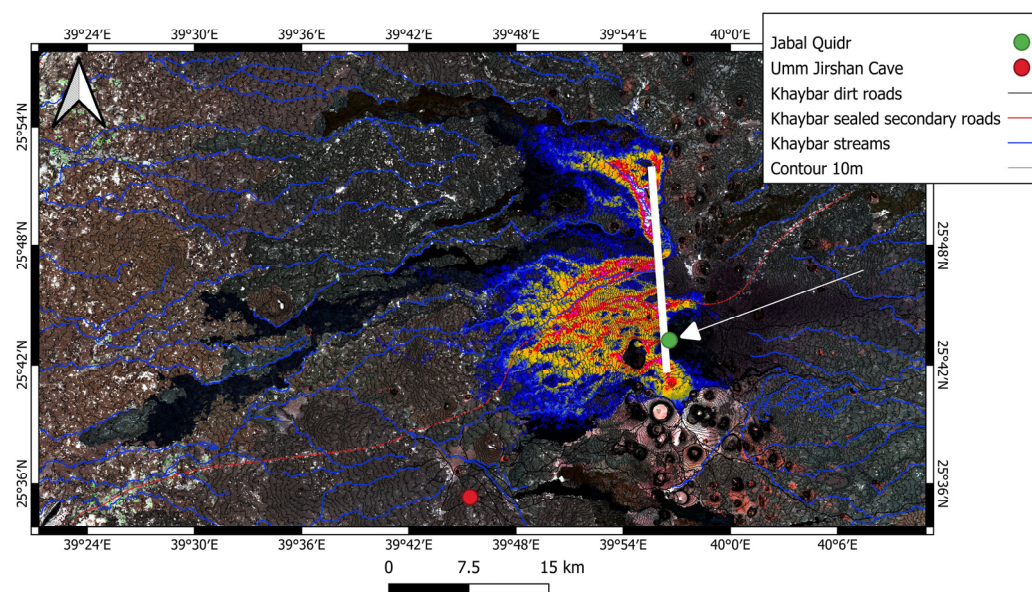


Figure 21. A long fissure simulation that operated by connecting Jabal Quidr (arrow) and the northern vents into a single long fissure, with eruption points spaced 500 m apart applying 500 km simulation distances, provided a very convincing lava flow inundation probability in the proximal regions, but again failed to offer inundation in distant regions.

5. Discussion

From our study, several important facts emerged that can be utilized for geoeducation and geotouristic development of the future of establishing a geopark within the volcanic field of Khaybar. Our terrain analysis and satellite image investigations revealed that the region is far gentler sloping than generally considered, but not yet explored. This terrain structure determines the lava flow emplacement nature. In the satellite images, long lava flows can reach over 50 km from their source, and they emplace in remarkable flat-floored stream valleys that are just several meters below the main eroded (weathered) old lava flow fields. The connection between the lava flow distribution and the preexisting stream valley network can be seen clearly in satellite images (Figure 22) in the distal regions. Interestingly, even in distal regions, lava flows can be seen as thin (dm to meter) sheets with micro-pāhoehoe surface textures following the narrow shallow wadis (Figure 22). In some cases, such pāhoehoe-type lavas seemingly initiated from rubble (‘a’ā-like channelized flows (Figure 22)), indicating that some flow “veins” must have been successfully tunneled through the otherwise rubbly piles of vesicular lava crust zones (Figure 22). This emplacement mechanism somehow differs from the traditional inflation and lava tube development model, and it is the likely indicator of specific conditions of steady supply of fresh lava that can retain heat over long distances and still be able to move relatively freely across the rubbly zones. This is not a typical emplacement mechanism associated with the general channel-filling ‘a’ā lava flow [85] or pāhoehoe flow emplacement. This transportation mechanism is inferred to operate by the ponding effect of melts in larger intersections of shallow valleys, where the accumulating melt can retain heat and keep lava ready to break out, forming its own skin that gradually moves into distal shallow stream valleys. Thin lava outbreaks are also common in the mid-distance zone where occasional faster moving and less viscous melt can be captured in side stream valleys that then can reunite downflow to the mainstream of the flow (Figure 23). In these zones, also, the rubbly, clastic flow channels coexist with more tube-like networks of melts (Figure 23). It was also demonstrated in the Laki Fissure eruption, where rubbly pāhoehoe flows commonly developed where, based on their crystallinity, their estimated cooling rate yielded only 0.3 degrees C/km, indicating that rubbly surfaced flows can be as thermally efficient as

tube-fed pāhoehoe lavas [96] and be able to keep melt at least in the base of the flow sheets, acting as a transport layer over a long time.

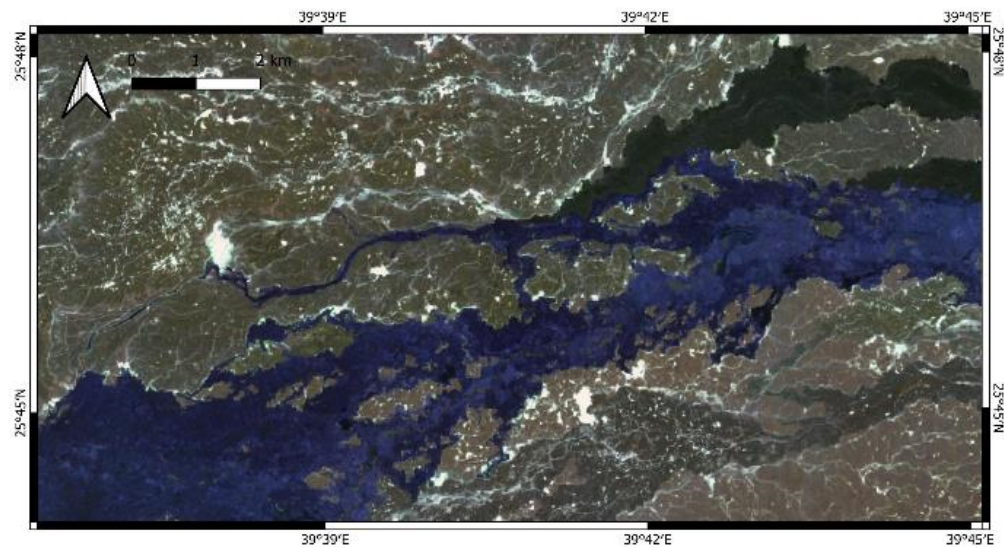


Figure 22. Typical distal lava flow field on a Sentinel SWIR satellite image clearly showing the narrow lava flow following a narrow and shallow dry valley within which it is captured. This narrow flow seemingly initiated from a ponded rubble pāhoehoe zone, suggesting ready squeeze-out flow to be moved further. Note the large, chilled lava crusts (bluish shiny zones) partially fragmented and rotated by the movement of the flow.

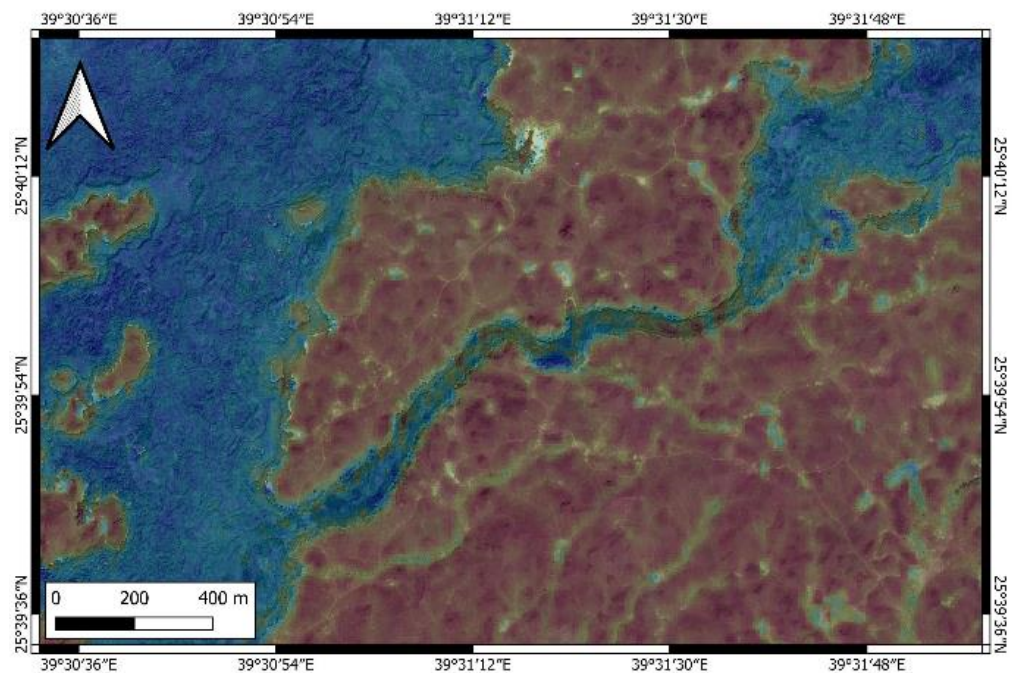


Figure 23. Narrow lava-tube-filled flow zone at mid-distance from the source of the lava on a Sentinel moisture index map. Note the less moist zones of the narrow lava flow, indicating some breakage of the lava crust and developing rubbly pāhoehoe that is reconnecting downflow with the main flow zone. Flow direction is from top to bottom.

One of the most intriguing flow textures recognized from the field are those distal narrow lava flows that are composed completely of rubbly pāhoehoe and 'a'ā-like abraded vesicular fragments. Interestingly, these zones also form sheet-like flat-topped zones, suggesting that the material moved within it more similar to a slow-moving mass flow.

The lack of evidence of bulldozing movement within these flows indicates a laminar transportation nature, keeping larger rubble intact and able to travel on the main body of the mass, instead of the common caterpillar effect that 'a'ā lava displays (Figure 24).

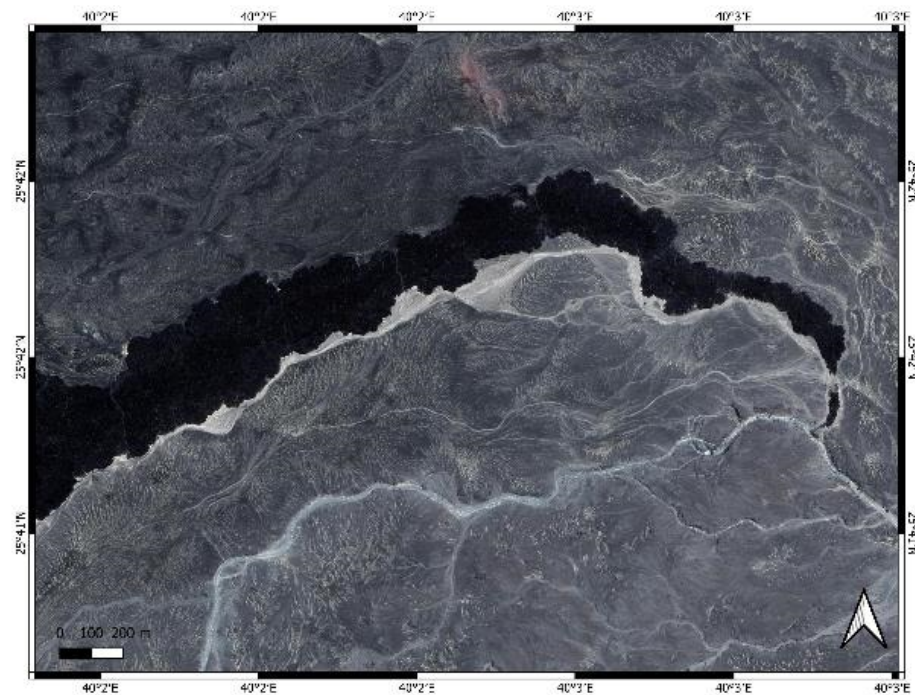


Figure 24. Gradually narrowing mass-flow-like lava flow terminus just east of the Jabal Quidr cone that was captured in a shallow wadi, similar to those visible in the Sentinel satellite image nearby.

The rubbly lava flows show remarkably uniform flat tops within which only few larger blocks are noted (Figure 25). Pressure ridges can be recognized as a reflection of the movement of the flow body gradually forced to remain in the shallow valleys (Figure 25).



Figure 25. Completely clastic type of lava flow section in the distal section of a lava flow east of Jabal Quidr. The lava flow left arm is about 300 m wide. It is very clear that the flow movement was heavily affected by the position of the microtopography.

Nearly all the observed medial or distal clastic lava flow zones formed flat-topped lava systems that spread across the entire available shallow channel network of the syneruptive topography. These flows are channelized and, by their emplacement, inferred to share common natures similar to many 'a'ā lavas. The rapid variation of the lava flow surface textures is inferred to be influenced by the influx of fresh, volatile-rich lava from the source, the microtopography, and the general slope angle of the terrain.

As Harrat Khaybar hosts large lava tubes, they are the proof that ponding and massive artery-like tube development took place in the evolution of the lava fields of Khaybar. This is very similar to those recorded from Jeju Island, South Korea, where large tubes effectively transported melts over long distances, and these sites currently form the bases of the Jeju Island UNESCO World Heritage Site [97]. Harrat Khaybar also shows similar facies architecture to other large lava-dominated intracontinental volcanic provinces such as those in southern Australia in the Newer Volcanics [98]. These regions also utilize their lava flow field heritage as a core of geotourism and geoeducation programs [99].

While Holocene volcanism is widespread and manifests as various types, geotourism that is structured or based on geopark programs is relatively rare. Volcanism and volcanic features commonly form the centerfold of local and global geopark programs in dormant or pre-Holocene volcanic terrains such as the monogenetic volcanic fields of western Germany [100,101], Central Europe [102,103], Taiwan [104], India [105], or in NE China [106]. These regions function very well as knowledge hubs disseminating aspects of volcanism and volcanic hazards. Among active volcanoes, or volcanoes known to have activity in the Holocene and form geoparks or other protected volcanic landscapes, the Canary Islands [107] provide excellent regions such as the El Hierro UNESCO Global Geopark [108] or El Teide National park in Tenerife [109]. Recent development also recognized the global significance of active volcanism beyond adventure tourism, and new proposals are emerging from regions previously not considered to demonstrate volcanic geodiversity, such as those regions in Eastern Turkey. Areas such as the Galapagos Islands, where biodiversity functions as a main magnet to drive tourism, are also increasingly utilizing the vast volcanic geoheritage that the region offers [110]. Volcanism is also a fundamental aspect of to link the natural environment to the society in regions where active volcanism is part of the life of the people but also acts as a magnet to attract visitors, such as those regions in Central America [111,112]. On active volcanoes, the volcanic hazard is an important aspect that geotourism needs to deal with to avoid deadly disasters [113] such as the Whakaari (White Island) 9 December 2019 eruption [114,115].

In addition, recently, the geoheritage values of dispersed or monogenetic volcanic fields were revisited and suggested to be used for natural hazard resilience [116–118]. Geotrails, explanatory panels, and geoeeducation centers were commonly suggested to be developed to raise public awareness of volcanism in such volcanic fields [119–121].

Volcanic fields such as the studied Harrat Khaybar, with their long eruption frequency (decades to millennia), however, clearly represent young volcanic terrains without the common visuals and experiences of active processes. They are, rather, volcanic terrains where fresh and young volcanic landforms can be viewed. In such terrains it is important that volcanic hazards such as lava flow inundation are studied, but, at the same time, the recorded information is directly fed into the geoeeducation programs. Geoparks in such terrains should, hence, function as a knowledge hub where volcanic hazard information and eruptive product preservation (e.g., lava flow heritage) together form strong geoeeducation for locals and visitors alike. Our work clearly demonstrates this potential pathway and provides valuable information for geopark developers in the region.

We also need to point out the limitations of our study. From the lava flow inundation perspective, it is important to point out that the available DEM resolution is 12.5 m, which is too coarse to truly model the lava flow moments at a fine scale. This is an important limitation as our observations also demonstrate that lava flows can be very thin (m-scale) in distal areas, and they tend to be very sensitive to microtopography at a scale of a few meters' elevation differences. Certainly, to capture lava flow movement and behavior at

such scale requires higher-resolution DEMs such as LiDAR-derived datasets. This could be an aim for future research. In addition, our work shows that the lava flows formed recently are very complex, and to calibrate modeling parameters, we probably need to look for simpler lava flows that future research will target. The lava flow inundation study can form fundamental core knowledge that can be included in the geoeducation program of the planned geopark of the region to demonstrate the lava flow behavior that we can expect in future eruptions.

From the geoconservation perspective, it is important to recognize the value of keeping these lava flows intact, as their preserved lava flow surface morphology is globally unique, while, being in an arid environment, also very fragile. Proper protection status and visitation management of the future geopark in the region should be coordinated with volcano experts.

6. Conclusions

In this report, we outlined the type of terrain in which Harrat Khaybar formed and released large volumes of lava. We demonstrated that lava flow emplacement in such gentle sloping terrains requires high magma flux rates, low viscosity, and high-temperature melts. We found that the lava flow simulations applying Q-LavHA produced good-probability maps for potential lava flow inundations in the proximal to medial zones but were not able to capture the full length of lava flows. We conclude that this might be the result of the frequent lava ponding in a topography step just west of the main vent axis of the field. In these areas, lava can accumulate and release more degassed melt further toward the distal zones that can form localized tubes and generate rubble zones, where sudden microrelief steps exist. Unfortunately, we must admit that the currently available DEM with 12.5 m resolution is probably not good enough to further refine the lava flow simulations. We found that the microreliefs that were able to control, divert, or repond lava were commonly significantly smaller than what the current DEM can capture. We also conclude that the identified lava flow textures and the Holocene eruption age of the fresh lava fields located in the center of development plans for geopark investment can be used for volcanic hazard education and would probably be a great attraction for geotourism ventures. As the volcanic field is an active field, but any future eruptions might be several generations away, the location can offer a very graphic picture of how volcanism occurred in the recent past in western Saudi Arabia, and of what we can expect in future volcanic unrest.

Author Contributions: Conceptualization, K.N.; methodology, K.N.; software, K.N.; validation, M.R.M.; formal analysis, K.N.; investigation, K.N. and M.R.M.; resources, M.R.M.; data curation, K.N.; writing—original draft preparation, K.N.; writing—review and editing, M.R.M.; visualization, K.N.; supervision, M.R.M.; project administration, M.R.M.; funding acquisition, M.R.M. All authors have read and agreed to the published version of the manuscript.

Funding: This research received no external funding.

Data Availability Statement: There is no publicly available dataset associated with this research.

Acknowledgments: This research enjoyed support from the Saudi Geological Survey.

Conflicts of Interest: The authors declare no conflict of interest.

References

1. Németh, K.; Casadevall, T.; Moufti, M.R.; Marti, J. Volcanic Geoheritage. *Geoheritage* **2017**, *9*, 251–254. [[CrossRef](#)]
2. Erfurt-Cooper, P. Geotourism in volcanic and geothermal environments: Playing with fire? *Geoheritage* **2011**, *3*, 187–193. [[CrossRef](#)]
3. Peterson, D.W.; Tilling, R.I. Lava flow hazards. In *Encyclopedia of Volcanoes*; Sigurdsson, H., Houghton, B.F., McNutt, S.R., Rymer, H., Stix, J., Eds.; Academic Press: San Diego, CA, USA, 2000; pp. 957–971.
4. Nakada, S. Hazards from pyroclastic flows and surges. In *Encyclopedia of Volcanoes*; Sigurdsson, H., Houghton, B.F., McNutt, S.R., Rymer, H., Stix, J., Eds.; Academic Press: San Diego, CA, USA, 2000; pp. 945–955.
5. Gudmundsson, M.T. Chapter 56—Hazards from Lahars and Jökulhlaups. In *The Encyclopedia of Volcanoes*, 2nd ed.; Sigurdsson, H., Ed.; Academic Press: Amsterdam, The Netherlands, 2015; pp. 971–984.
6. Cashman, K.V.; Sparks, R.S.J. How volcanoes work: A 25 year perspective. *Geol. Soc. Am. Bull.* **2013**, *125*, 664–690. [[CrossRef](#)]

7. Dibben, C.; Chester, D.K. Human vulnerability in volcanic environments: The case of Furnas, Sao Miguel, Azores. *J. Volcanol. Geotherm. Res.* **1999**, *92*, 133–150. [[CrossRef](#)]
8. McGuire, W.J.; Kilburn, C.R.J. Forecasting volcanic events: Some contemporary issues. *Geol. Rundsch.* **1997**, *86*, 439–445. [[CrossRef](#)]
9. Scarlett, J.P.; Riede, F. The Dark Geocultural Heritage of Volcanoes: Combining Cultural and Geoheritage Perspectives for Mutual Benefit. *Geoheritage* **2019**, *11*, 1705–1721. [[CrossRef](#)]
10. Németh, K. Geoheritage and geodiversity aspects of catastrophic volcanic eruptions: Lessons from the 15th of January 2022 Hunga Tonga—Hunga Ha’apai eruption, SW Pacific. *Int. J. Geoheritage Park.* **2022**, *10*, 546–568. [[CrossRef](#)]
11. Reynard, E.; Giusti, C. Chapter 8—The Landscape and the Cultural Value of Geoheritage. In *Geoheritage*; Reynard, E., Brilha, J., Eds.; Elsevier: Amsterdam, The Netherlands, 2018; pp. 147–166.
12. Szepesi, J.; Esik, Z.; Soos, I.; Németh, B.; Suto, L.; Novak, T.J.; Harangi, S.; Lukacs, R. Identification of Geoheritage Elements in a Cultural Landscape: A Case Study from Tokaj Mts, Hungary. *Geoheritage* **2020**, *12*, 89. [[CrossRef](#)]
13. Németh, K.; Gravis, I. Geoheritage and geodiversity elements of the SW Pacific: A conceptual framework. *Int. J. Geoheritage Park.* **2022**, *10*, 523–545. [[CrossRef](#)]
14. Dull, R.A.; Southon, J.R.; Sheets, P. Volcanism, ecology and culture: A reassessment of the Volcan Ilopango TBJ eruption in the southern Maya realm. *Lat. Am. Antiq.* **2001**, *12*, 25–44. [[CrossRef](#)]
15. Ertekin, C.; Ekinci, Y.L.; Buyuksarac, A.; Ekinci, R. Geoheritage in a Mythical and Volcanic Terrain: An Inventory and Assessment Study for Geopark and Geotourism, Nemrut Volcano (Bitlis, Eastern Turkey). *Geoheritage* **2021**, *13*, 73. [[CrossRef](#)]
16. Erturac, M.K.; Okur, H.; Ersoy, B. The cultural and geological heritage sites within the Golludag Volcanic Complex. *Turk. Jeol. Bul. Geol. Bull. Turk.* **2017**, *60*, 17–34. [[CrossRef](#)]
17. Moufti, M.R.; Németh, K. The intra-continental Al Madinah Volcanic Field, Western Saudi Arabia: A proposal to establish harrat Al Madinah as the first volcanic geopark in the Kingdom of Saudi Arabia. *Geoheritage* **2013**, *5*, 185–206. [[CrossRef](#)]
18. Wilkie, B.; Cahir, F.; Clark, I.D. Volcanism in Aboriginal Australian oral traditions: Ethnographic evidence from the Newer Volcanics Province. *J. Volcanol. Geotherm. Res.* **2020**, *403*, 106999. [[CrossRef](#)]
19. Riede, F.; Barnes, G.L.; Elson, M.D.; Oetelaar, G.A.; Holmberg, K.G.; Sheets, P. Prospects and pitfalls in integrating volcanology and archaeology: A review. *J. Volcanol. Geotherm. Res.* **2020**, *401*, 106977. [[CrossRef](#)]
20. Németh, K. Volcanic Geoheritage in the Light of Volcano Geology. In *El Hierro Island Global Geopark: Diversity of Volcanic Heritage for Geotourism*; Dóniz-Páez, J., Pérez, N.M., Eds.; Springer International Publishing: Cham, Switzerland, 2023; pp. 1–24.
21. Migon, P.; Pijet-Migon, E. Overlooked geomorphological component of volcanic geoheritage-diversity and perspectives for tourism industry, Pogrze Kaczawskie Region, SW Poland. *Geoheritage* **2016**, *8*, 333–350. [[CrossRef](#)]
22. Szepesi, J.; Harangi, S.; Esik, Z.; Novak, T.J.; Lukacs, R.; Soos, I. Volcanic Geoheritage and Geotourism Perspectives in Hungary: A Case of an UNESCO World Heritage Site, Tokaj Wine Region Historic Cultural Landscape, Hungary. *Geoheritage* **2017**, *9*, 329–349. [[CrossRef](#)]
23. Rapprich, V.; Lisec, M.; Fiferna, P.; Závada, P. Application of Modern Technologies in Popularization of the Czech Volcanic Geoheritage. *Geoheritage* **2017**, *9*, 413–420. [[CrossRef](#)]
24. Migon, P.; Pijet-Migon, E. Bakony—Balaton Geopark in Hungary. *Przegląd Geologiczny* **2018**, *66*, 276–283.
25. Pal, M.; Albert, G. Examining the Spatial Variability of Geosite Assessment and Its Relevance in Geosite Management. *Geoheritage* **2021**, *13*, 8. [[CrossRef](#)]
26. Ruban, D.A.; Ermolaev, V.A.; van Loon, A.J. Better Understanding of Geoheritage Challenges within the Scope of Economic Geology: Toward a New Research Agenda. *Heritage* **2023**, *6*, 365–373. [[CrossRef](#)]
27. Chakraborty, A.; Cooper, M.; Chakraborty, S. Geosystems as a Framework for Geoconservation: The Case of Japan’s Izu Peninsula Geopark. *Geoheritage* **2015**, *7*, 351–363. [[CrossRef](#)]
28. van Ree, C.C.D.F.; van Beukering, P.J.H. Geosystem services: A concept in support of sustainable development of the subsurface. *Ecosyst. Serv.* **2016**, *20*, 30–36. [[CrossRef](#)]
29. Brocx, M.; Semeniuk, V.; Casadevall, T.J.; Tormey, D. Volcanoes: Identifying and Evaluating Their Significant Geoheritage Features from the Large to Small Scale. In *Updates in Volcanology—Transdisciplinary Nature of Volcano Science*; Németh, K., Ed.; IntechOpen: Rijeka, Croatia, 2021; pp. 329–346. [[CrossRef](#)]
30. Brocx, M.; Semeniuk, V. Using the Geoheritage Tool-Kit to Identify Inter-related Geological Features at Various Scales for Designating Geoparks: Case Studies from Western Australia. In *From Geoheritage to Geoparks: Case Studies from Africa and Beyond*; Geoheritage Geoparks and Geotourism; Errami, E., Brocx, M., Semeniuk, V., Eds.; Springer: Berlin/Heidelberg, Germany, 2015; pp. 245–259.
31. Németh, K.; Moufti, M.R. Geoheritage values of a mature monogenetic volcanic field in intra-continental settings: Harrat Khaybar, Kingdom of Saudi Arabia. *Geoheritage* **2017**, *9*, 311–328. [[CrossRef](#)]
32. Naseem, S. The role of tourism in economic growth: Empirical evidence from Saudi Arabia. *Economies* **2021**, *9*, 117. [[CrossRef](#)]
33. Ibrahim, A.O.; Baqawy, G.A.; Mohamed, M.A.S. Tourism attraction sites: Boasting the booming tourism of Saudi Arabia. *Int. J. Adv. Appl. Sci.* **2021**, *8*, 1–11. [[CrossRef](#)]
34. Al Mohaya, J.; Elassal, M. Assessment of Geosites and Geotouristic Sites for Mapping Geotourism: A Case Study of Al-Soudah, Asir Region, Saudi Arabia. *Geoheritage* **2023**, *15*, 7. [[CrossRef](#)]

35. Al-Hashim, M.H.; El-Asmar, H.M.; Hereher, M.E.; Alshehri, F. Sedimentomorphic geodiversity in response to depositional environments: Remote sensing application along the coastal plain between Ummlujj and Al-Wajh, Red Sea, Saudi Arabia. *Arab. J. Geosci.* **2021**, *14*, 1061. [[CrossRef](#)]
36. Ellassal, M. Geomorphological Heritage Attractions Proposed for Geotourism in Asir Mountains, Saudi Arabia. *Geoheritage* **2020**, *12*, 78. [[CrossRef](#)]
37. Hassan, T.; Carvache-Franco, M.; Carvache-Franco, W.; Carvache-Franco, O. Segmentation of Religious Tourism by Motivations: A Study of the Pilgrimage to the City of Mecca. *Sustainability* **2022**, *14*, 7861. [[CrossRef](#)]
38. Wided, R. Achieving sustainable tourism with dynamic capabilities and resilience factors: A post disaster perspective case of the tourism industry in Saudi Arabia. *Cogent Soc. Sci.* **2022**, *8*, 2060539. [[CrossRef](#)]
39. Supriadi, U.; Islamy, M.R.F.; Rakhman, M.A.; Fuadin, A. Tourism and Crisis: Comparing the Impacts of COVID-19 and Natural Disasters on The Hajj and Umrah Industry. *Int. J. Relig. Tour. Pilgr.* **2022**, *10*, 2. [[CrossRef](#)]
40. Alkhalwaldeh, A.M. Religious Tourism Post-COVID-19 In The Context Of Muslim Countries: Destination Image, Perceived Value, Intention To Revisit Makkah And Health Risk As Moderator. *Geoj. Tour. Geosites* **2022**, *43*, 858–865. [[CrossRef](#)]
41. Yehia, E.F.; Alzahrani, H.J.M.; Reid, D.M.; Ali, M.A. Tourism, national identity, and the images on postage stamps: The case of Saudi Arabia. *J. Tour. Hist.* **2022**, *14*, 70–102. [[CrossRef](#)]
42. Elbelkasy, M.I.; Mustafa, M.M.I. Investment of Heritage Villages in Saudi Arabia—Case Study of Al-Khubara Village in Qassim. *Adv. Sci. Technol. Innov.* **2022**, *345*–356. [[CrossRef](#)]
43. Rehman, A.U.; Alnuzhah, A.S. Identifying Travel Motivations Of Saudi Domestic Tourists: Case of Hail Province in Saudi Arabia. *Geoj. Tour. Geosites* **2022**, *43*, 1118–1128. [[CrossRef](#)]
44. Mazetto, S. Sustainable Heritage Preservation to Improve the Tourism Offer in Saudi Arabia. *Urban Planning* **2022**, *7*, 195–207. [[CrossRef](#)]
45. Bay, M.A.; Alnaim, M.M.; Albaqawy, G.A.; Noaime, E. The Heritage Jewel of Saudi Arabia: A Descriptive Analysis of the Heritage Management and Development Activities in the At-Turaif District in Ad-Dir'iyah, a World Heritage Site (WHS). *Sustainability* **2022**, *14*, 10718. [[CrossRef](#)]
46. Madani, R. The new image of Saudi cultural shift; MDL Beast music festival; Saudi Vision 2030. *Cogent Arts Humanit.* **2022**, *9*, 2105511. [[CrossRef](#)]
47. Hind, K. Saudi Vision 2030: Applying a Sustainable Smart Techno-cultural Assessment method to Evaluate Museums' performance post-COVID-19. In *Proceedings of the IOP Conference Series: Earth and Environmental Science*; IOP Publishing: Bristol, UK, 2022.
48. Greco, C. Food Heritage, Memory and Cultural Identity in Saudi Arabia: The Case of Jeddah. *Numanities Arts Humanit. Prog.* **2022**, *19*, 55–74. [[CrossRef](#)]
49. Aliraqi, A.M. Heritage-based Entertainment: Empirical Evidence from Diriyah, Saudi Arabia. *World J. Entrep. Manag. Sustain. Dev.* **2022**, *18*, 467–480. [[CrossRef](#)]
50. Hassan, T.H.; Salem, A.E.; Abdelmoaty, M.A.; Saleh, M.I. Renewing The Ecotourism Investments' Strategies In The Kingdom of Saudi Arabia: Social Exchange Theory Prospects. *Geoj. Tour. Geosites* **2022**, *45*, 1661–1673. [[CrossRef](#)]
51. Hassan, T.H.; Salem, A.E.; Abdelmoaty, M.A. Impact of Rural Tourism Development on Residents' Satisfaction with the Local Environment, Socio-Economy and Quality of Life in Al-Ahsa Region, Saudi Arabia. *Int. J. Environ. Res. Public Health* **2022**, *19*, 4410. [[CrossRef](#)]
52. Faraj, T.K.; Tarawneh, Q.Y.; Oroud, I.M. The applicability of the tourism climate index in a hot arid environment: Saudi Arabia as a case study. *Int. J. Environ. Sci. Technol.* **2022**, *20*, 3849–3860. [[CrossRef](#)]
53. Fagehi, H.; Hadidi, H.M. Toward buildings with lower power demand in the smart city of NEOM-incorporating phase change material into building envelopes. *Sustain. Energy Technol. Assess.* **2022**, *53*, 102494. [[CrossRef](#)]
54. Fu, H.; Fu, B.; Shi, P.; Zheng, Y. International geological significance of the potential Al-Medina volcanic UNESCO Global Geopark Project in Saudi Arabia revealed from multi-satellite remote sensing data. *Herit. Sci.* **2021**, *9*, 149. [[CrossRef](#)]
55. Moufti, M.R.; Németh, K. *Geoheritage of Volcanic Harrats in Saudi Arabia*; Springer: Heidelberg, Germany, 2016; pp. 1–194.
56. Németh, K.; Kereszturi, G. Monogenetic volcanism: Personal views and discussion. *Int. J. Earth Sci.* **2015**, *104*, 2131–2146. [[CrossRef](#)]
57. Camp, V.E.; Roobol, M.J.; Hooper, P.R. The Arabian Continental Alkali Basalt Province 2. Evolution of Harrats Khaybar, Ithnayn, and Kura, Kingdom of Saudi-Arabia. *Geol. Soc. Am. Bull.* **1991**, *103*, 363–391. [[CrossRef](#)]
58. Németh, K.; Moufti, M.R. The historic scoria cone of Jabal Quidr, Saudi Arabia. In *The First 100 UGS Geological Heritage Sites*; Hilario, A., Asrat, A., van Wyk de Vries, B., Mogk, D., Lozano, G., Zhang, J., Brilha, J., Vegas, J., Lemon, K., Carcavilla, L., et al., Eds.; International Union of Geological Sciences: Zumaia, Spain, 2022; pp. 150–151.
59. Stelten, M.E.; Downs, D.T.; Champion, D.E.; Dietterich, H.R.; Calvert, A.T.; Sisson, T.W.; Mahood, G.A.; Zahran, H. The timing and compositional evolution of volcanism within northern Harrat Rahat, Kingdom of Saudi Arabia. *Bull. Geol. Soc. Am.* **2020**, *132*, 1381–1403. [[CrossRef](#)]
60. Downs, D.T.; Stelten, M.E.; Champion, D.E.; Dietterich, H.R.; Nawab, Z.; Zahran, H.; Hassan, K.; Shawali, J. Volcanic history of the northernmost part of the Harrat Rahat volcanic field, Saudi Arabia. *Geosphere* **2018**, *14*, 1253–1282. [[CrossRef](#)]

61. Moufti, M.R.; Moghazi, A.M.; Ali, K.A. $^{40}\text{Ar}/^{39}\text{Ar}$ geochronology of the Neogene-Quaternary Harrat Al-Madinah intercontinental volcanic field, Saudi Arabia: Implications for duration and migration of volcanic activity. *J. Asian Earth Sci.* **2013**, *62*, 253–268. [[CrossRef](#)]
62. Downs, D.T.; Robinson, J.E.; Stelten, M.E.; Champion, D.E.; Dietterich, H.R.; Sisson, T.W.; Zahran, H.; Hassan, K.; Shawali, J. *Geologic Map of the Northern Harrat Rahat Volcanic Field, Kingdom of Saudi Arabia*; 3428; US Department of the Interior, US Geological Survey: Reston, VA, USA, 2019; p. 62.
63. Walker, M.; Head, M.J.; Lowe, J.; Berkelhammer, M.; Björck, S.; Cheng, H.; Cwynar, L.C.; Fisher, D.; Gkinis, V.; Long, A.; et al. Subdividing the Holocene Series/Epoch: Formalization of stages/ages and subseries/subepochs, and designation of GSSPs and auxiliary stratotypes. *J. Quat. Sci.* **2019**, *34*, 173–186. [[CrossRef](#)]
64. Camp, V.E.; Hooper, P.R.; Roobol, M.J.; White, D.L. The Madinah eruption, Saudi Arabia: Magma mixing and simultaneous extrusion of three basaltic chemical types. *Bull. Volcanol.* **1987**, *49*, 489–508. [[CrossRef](#)]
65. Moufti, M.R.; Németh, K. The White Mountains of Harrat Khaybar, Kingdom of Saudi Arabia. *Int. J. Earth Sci.* **2014**, *103*, 1641–1643. [[CrossRef](#)]
66. Moufti, M.R.; Németh, K.; El-Masry, N.; Qaddah, A. Geoheritage values of one of the largest maar craters in the Arabian Peninsula: The Al Wahbah Crater and other volcanoes (Harrat Kishb, Saudi Arabia). *Cent. Eur. J. Geosci.* **2013**, *5*, 254–271. [[CrossRef](#)]
67. Jasiewicz, J.; Stepinski, T.F. Geomorphons—A pattern recognition approach to classification and mapping of landforms. *Geomorphology* **2013**, *182*, 147–156. [[CrossRef](#)]
68. Kim, D.-E.; Seong, Y.B.; Sohn, H.; Choi, K. Landform Classification using Geomorphons. *J. Korean Geomorphol. Assoc.* **2012**, *19*, 139–155.
69. Kempe, S.; Al-Malabeh, A. Desert kites in Jordan and Saudi Arabia: Structure, statistics and function, a Google Earth study. *Quat. Int.* **2013**, *297*, 126–146. [[CrossRef](#)]
70. Barge, O.; Brochier, J.E.; Régagnon, E.; Chambrade, M.-L.; Crassard, R. Unity and diversity of the kite phenomenon: A comparative study between Jordan, Armenia and Kazakhstan. *Arab. Archaeol. Epigr.* **2015**, *26*, 144–161. [[CrossRef](#)]
71. Repper, R.; Kennedy, M.; McMahon, J.; Boyer, D.; Dalton, M.; Thomas, H.; Kennedy, D. Kites of AlUla County and the Harrat 'Uwayrid, Saudi Arabia. *Arab. Archaeol. Epigr.* **2022**, *33*, 3–22. [[CrossRef](#)]
72. Bouzid, S.; Barge, O. Towards a typology of desert kites combining quantitative and spatial approaches. *Archaeol. Anthropol. Sci.* **2022**, *14*, 91. [[CrossRef](#)]
73. Fradley, M.; Simi, F.; Guagnin, M. Following the herds? A new distribution of hunting kites in Southwest Asia. *Holocene* **2022**, *32*, 1160–1172. [[CrossRef](#)]
74. Crassard, R.; Abu-Azizeh, W.; Barge, O.; Brochier, J.É.; Chahoud, J.; Régagnon, E. The Use of Desert Kites as Hunting Mega-Traps: Functional Evidence and Potential Impacts on Socioeconomic and Ecological Spheres. *J. World Prehistory* **2022**, *35*, 1–44. [[CrossRef](#)]
75. Barge, O.; Balaresque, L.; Baudoin, J.L.; Boelke, M.; Derrien, L. Hunting in the desert: Assessing the form and use of kite-like structures in the western Sahara. *Antiquity* **2022**, *96*, 719–726. [[CrossRef](#)]
76. Barge, O.; Albukaai, D.; Boelke, M.; Guadagnini, K.; Régagnon, E.; Crassard, R. New Arabian desert kites and potential proto-kites extend the global distribution of hunting mega-traps. *J. Archaeol. Sci. Rep.* **2022**, *42*, 103403. [[CrossRef](#)]
77. Groucutt, H.S.; Carleton, W.C. Mass-kill hunting and Late Quaternary ecology: New insights into the 'desert kite' phenomenon in Arabia. *J. Archaeol. Sci. Rep.* **2021**, *37*, 102995. [[CrossRef](#)]
78. Lombard, M.; Badenhorst, S. A Case for Springbok Hunting with Kite-Like Structures in the Northwest Nama Karoo Bioregion of South Africa. *Afr. Archaeol. Rev.* **2019**, *36*, 383–396. [[CrossRef](#)]
79. Giannelli, G.; Maestrucci, F. Desert kites in the Tripolitania region: New evidence from satellite imagery. *Antiquity* **2019**, *93*, e26. [[CrossRef](#)]
80. Brunner, U. Desert kites—Old structures, new research. *Arab. Archaeol. Epigr.* **2015**, *26*, 70–73. [[CrossRef](#)]
81. Kennedy, D. Kites—New discoveries and a new type. *Arab. Archaeol. Epigr.* **2012**, *23*, 145–155. [[CrossRef](#)]
82. Felpeto, A.; Araña, V.; Ortiz, R.; Astiz, M.; García, A. Assessment and modelling of lava flow hazard on Lanzarote (Canary Islands). *Nat. Hazards* **2001**, *23*, 247–257. [[CrossRef](#)]
83. Harris, A.J.L.; Rowland, S.K. FLOWGO: A kinematic thermo-rheological model for lava flowing in a channel. *Bull. Volcanol.* **2001**, *63*, 20–44. [[CrossRef](#)]
84. Dille, A.; Poppe, S.; Mossoux, S.; Soule, H.; Kervyn, M. Modeling Lahars on a Poorly Eroded Basaltic Shield: Karthala Volcano, Grande Comore Island. *Front. Earth Sci.* **2020**, *8*. [[CrossRef](#)]
85. Rodríguez-González, A.; Aulinas, M.; Mossoux, S.; Pérez-Torrado, F.J.; Fernández-Turiel, J.L.; Cabrera, M.; Prieto-Torrell, C. Comparison of real and simulated lava flows in the Holocene volcanism of Gran Canaria (Canary Islands, Spain) with Q-LavHA: Contribution to volcanic hazard management. *Nat. Hazards* **2021**, *107*, 1785–1819. [[CrossRef](#)]
86. Vilches, M.; Ureta, G.; Grosse, P.; Németh, K.; Aguilera, F.; Aguilera, M. Effusion rate estimation based on solidified lava flows: Implications for volcanic hazard assessment in the Negros de Aras monogenetic volcanic field, northern Chile. *J. Volcanol. Geotherm. Res.* **2022**, *422*, 107454. [[CrossRef](#)]
87. Becerril, L.; Larrea, P.; Salinas, S.; Mossoux, S.; Ferres, D.; Widom, E.; Siebe, C.; Marti, J. The historical case of Parícutin volcano (Michoacan, Mexico): Challenges of simulating lava flows on a gentle slope during a long-lasting eruption. *Nat. Hazards* **2021**, *107*, 809–829. [[CrossRef](#)]

88. Diniega, S.; Németh, K. Tumulus. In *Encyclopedia of Planetary Landforms*; Hargitai, H., Kereszturi, Á., Eds.; Springer New York: New York, NY, USA, 2015; pp. 2210–2214.
89. Fodor, E.; Németh, K. Spatter Cone. In *Encyclopedia of Planetary Landforms*; Hargitai, H., Kereszturi, Á., Eds.; Springer New York: New York, NY, USA, 2015; pp. 2028–2034.
90. Pedersen, G.B.M.; Hoskuldsson, A.; Durig, T.; Thordarson, T.; Jonsdottir, I.; Riishuus, M.S.; Oskarsson, B.V.; Dumont, S.; Magnusson, E.; Gudmundsson, M.T.; et al. Lava field evolution and emplacement dynamics of the 2014–2015 basaltic fissure eruption at Holuhraun, Iceland. *J. Volcanol. Geotherm. Res.* **2017**, *340*, 155–169. [[CrossRef](#)]
91. Murcia, H.; Németh, K.; Moufti, M.R.; Lindsay, J.M.; El-Masry, N.; Cronin, S.J.; Qaddah, A.; Smith, I.E.M. Late Holocene lava flow morphotypes of northern Harrat Rahat, Kingdom of Saudi Arabia: Implications for the description of continental lava fields. *J. Asian Earth Sci.* **2014**, *84*, 131–145. [[CrossRef](#)]
92. Pint, J.J. Umm Jirsan: Arabia's longest lava tube system. In *Proceedings of the International Congress of Speleology*; National Speleological Society: Kerrville, TX, USA, 2009; Volume 2, pp. 714–717.
93. Pint, J.J. The lava caves of Khaybar, Saudi Arabia. In *Proceedings of the International Congress of Speleology*; National Speleological Society: Kerrville, TX, USA, 2009; Volume 3, pp. 1873–1878.
94. Nicholson, S.L.; Pike, A.W.G.; Hosfield, R.; Roberts, N.; Sahy, D.; Woodhead, J.; Cheng, H.; Edwards, R.L.; Affolter, S.; Leuenberger, M.; et al. Pluvial periods in Southern Arabia over the last 1.1 million-years. *Quat. Sci. Rev.* **2020**, *229*, 106112. [[CrossRef](#)]
95. Preston, G.W.; Parker, A.G. Understanding the evolution of the Holocene Pluvial Phase and its impact on Neolithic populations in south-east Arabia. *Arab. Archaeol. Epigr.* **2013**, *24*, 87–94. [[CrossRef](#)]
96. Guilbaud, M.N.; Blake, S.; Thordarson, T.; Self, S. Role of syn-eruptive cooling and degassing on textures of lavas from the AD 1783–1784 Laki eruption, south Iceland. *J. Petrol.* **2007**, *48*, 1265–1294. [[CrossRef](#)]
97. Woo, K.S.; Kim, L.; Ji, H.; Jeon, Y.; Ryu, C.G.; Wood, C. Geological Heritage Values of the Yongcheon Cave (Lava Tube Cave), Jeju Island, Korea. *Geoheritage* **2019**, *11*, 615–628. [[CrossRef](#)]
98. Hare, A.G.; Cas, R.A.F. Volcanology and evolution of the Werribee Plains intraplate, basaltic lava flow-field, Newer Volcanics Province, southeast Australia. *Aust. J. Earth Sci.* **2005**, *52*, 59–78. [[CrossRef](#)]
99. Joyce, E. Australia's Geoheritage: History of Study, A New Inventory of Geosites and Applications to Geotourism and Geoparks. *Geoheritage* **2010**, *2*, 39–56. [[CrossRef](#)]
100. Megerle, H.E. Geoheritage and geotourism in regions with extinct volcanism in Germany; case study Southwest Germany with UNESCO global Geopark Swabian Alb. *Geosciences* **2020**, *10*, 445. [[CrossRef](#)]
101. Bitschene, P.R. Edutainment with basalt and volcanoes—The rockskyller kopf example in the westeifel volcanic field/vulkaneifel european geopark, Germany. *Z. Der Dtsch. Ges. Fur Geowiss.* **2015**, *166*, 187–193. [[CrossRef](#)]
102. Migoñ, P.; Pijet-Migoñ, E. Late Palaeozoic Volcanism in Central Europe—Geoheritage Significance and Use in Geotourism. *Geoheritage* **2020**, *12*, 43. [[CrossRef](#)]
103. Harangi, S. Volcanic heritage of the carpathian-pannonian region in eastern-central Europe. In *Volcanic Tourist Destinations*; Springer Science & Business Media: Berlin, Germany, 2014; pp. 103–123.
104. Migoñ, P. Geoparks and geotourism in Taiwan. *Prz. Geol.* **2012**, *60*, 315–318.
105. Sheth, H.; Samant, H.; Patel, V.; D'Souza, J. The Volcanic Geoheritage of the Elephanta Caves, Deccan Traps, Western India. *Geoheritage* **2017**, *9*, 359–372. [[CrossRef](#)]
106. Németh, K.; Wu, J.; Sun, C.; Liu, J. Update on the Volcanic Geoheritage Values of the Pliocene to Quaternary Arxan–Chaihe Volcanic Field, Inner Mongolia, China. *Geoheritage* **2017**, *9*, 279–297. [[CrossRef](#)]
107. Dóniz-Páez, J.; Beltrán-Yanes, E.; Becerra-Ramírez, R.; Pérez, N.M.; Hernández, P.A.; Hernández, W. Diversity of volcanic geoheritage in the canary islands, Spain. *Geosciences* **2020**, *10*, 390. [[CrossRef](#)]
108. Dóniz Páez, J.; Becerra-Ramírez, R.; Beltrán Yanes, E. Geomorphosites of El Hierro global Unesco geopark (Canary Islands, Spain) to promote the volcanic geotourism. *Rev. De Geogr. Norte Gd.* **2021**, *2021*, 165–186. [[CrossRef](#)]
109. Martí-Molist, J.; Dorado-García, O.; López-Saavedra, M. The Volcanic Geoheritage of El Teide National Park (Tenerife, Canary Islands, Spain). *Geoheritage* **2022**, *14*, 65. [[CrossRef](#)]
110. Kelley, D.; Salazar, R. Geosites in the Galápagos Islands Used for Geology Education Programs. *Geoheritage* **2017**, *9*, 351–358. [[CrossRef](#)]
111. Quesada-Román, A.; Pérez-Umaña, D. State of the art of geodiversity, geoconservation, and geotourism in Costa Rica. *Geosciences* **2020**, *10*, 211. [[CrossRef](#)]
112. Quesada-Román, A.; Torres-Bernhard, L.; Ruiz-álvarez, M.A.; Rodríguez-Maradiaga, M.; Velázquez-Espinoza, G.; Espinosa-Vega, C.; Toral, J.; Rodríguez-Bolaños, H. Geodiversity, Geoconservation, and Geotourism in Central America. *Land* **2022**, *11*, 48. [[CrossRef](#)]
113. Erfurt, P. Volcano Tourism and Visitor Safety: Still Playing with Fire? A 10-Year Update. *Geoheritage* **2022**, *14*, 56. [[CrossRef](#)]
114. Kilgour, G.; Kennedy, B.; Scott, B.; Christenson, B.; Jolly, A.; Asher, C.; Rosenberg, M.; Saunders, K. Whakaari/White Island: A review of New Zealand's most active volcano. *New Zealand J. Geol. Geophys.* **2021**, *64*, 273–295. [[CrossRef](#)]
115. Burton, M.; Hayer, C.; Miller, C.; Christenson, B. Insights into the 9 December 2019 eruption of Whakaari/White Island from analysis of TROPOMI SO₂ imagery. *Sci. Adv.* **2021**, *7*. [[CrossRef](#)]
116. Guilbaud, M.-N.; Ortega-Larrocea, M.d.P.; Cram, S.; van Wyk de Vries, B. Xitle Volcano Geoheritage, Mexico City: Raising Awareness of Natural Hazards and Environmental Sustainability in Active Volcanic Areas. *Geoheritage* **2021**, *13*, 6. [[CrossRef](#)]

117. Planagumà, L.; Martí, J. Identification, cataloguing and preservation of outcrops of geological interest in monogenetic volcanic fields: The case of La Garrotxa Volcanic Zone Natural Park. *Geoheritage* **2020**, *12*, 84. [[CrossRef](#)]
118. Planagumà-Guardia, L.; Martí-Molist, J.; Vila-Subirós, J. Conservation of the Geological Heritage of Volcanic Fields: La Garrotxa Volcanic Zone Natural Park, Spain. *Geoheritage* **2022**, *14*, 39. [[CrossRef](#)]
119. Alberico, I.; Alessio, G.; Fagnano, M.; Petrosino, P. The Effectiveness of Geotrails to Support Sustainable Development in the Campi Flegrei Active Volcanic Area. *Geoheritage* **2022**, *15*, 15. [[CrossRef](#)]
120. Gravis, I.; Németh, K.; Twemlow, C.; Németh, B. The Case for Community-Led Geoheritage and Geoconservation Ventures in Mangere, South Auckland, and Central Otago, New Zealand. *Geoheritage* **2020**, *12*, 19. [[CrossRef](#)]
121. Németh, B.; Németh, K.; Procter, J.N. Visitation rate analysis of geoheritage features from earth science education perspective using automated landform classification and crowdsourcing: A geoeducation capacity map of the Auckland Volcanic Field, New Zealand. *Geosciences* **2021**, *11*, 480. [[CrossRef](#)]

Disclaimer/Publisher's Note: The statements, opinions and data contained in all publications are solely those of the individual author(s) and contributor(s) and not of MDPI and/or the editor(s). MDPI and/or the editor(s) disclaim responsibility for any injury to people or property resulting from any ideas, methods, instructions or products referred to in the content.